A cell-based model of extracellular-matrix-guided endothelial cell migration during angiogenesis

MSc thesis

Author:

Josephine Daub

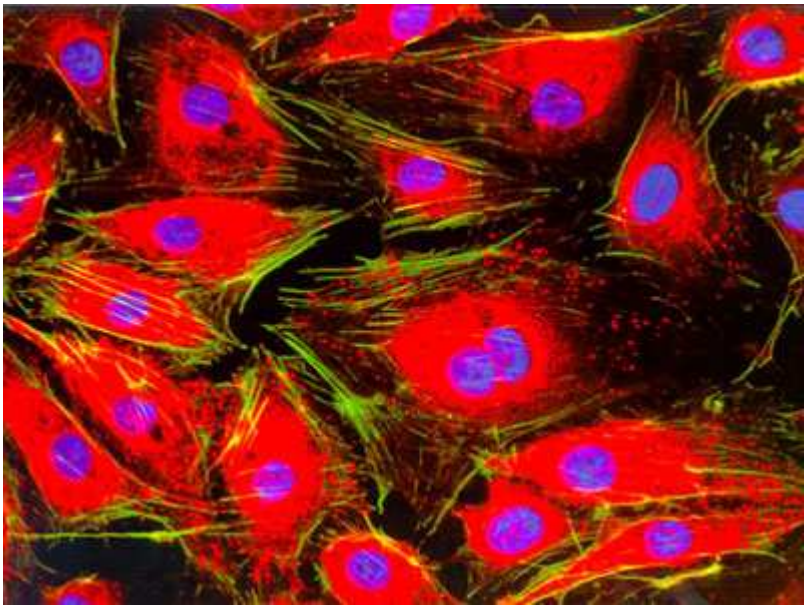

June 2010

A cell-based model of extracellular-matrix-guided endothelial cell migration during angiogenesis

Author:

Josephine Daub

Supervisors:

Dr. Jaap Kaandorp

Dr. Roeland Merks

Committee members:

Dr. Inge Bethke

Dr. Jaap Kaandorp

Dr. Roeland Merks

Carlos Tamulonis (MSc)

Submitted to the Faculty of Science in partial fulfillment of the requirements for the degree of Master of Science in Grid Computing (Track Computational Science)

UNIVERSITEIT VAN AMSTERDAM

June 2010

Cover page:
Endothelial cells, picture taken by Jakob Zbaeren, Insel Hospital, Bern, Switzerland.

Winning picture at the 1998 Nikon Small World Contest
http://www.nikonsmallworld.com/gallery/year/1998/1

Abstract

Angiogenesis, the formation of new blood vessels sprouting from existing ones, occurs in several situations like wound healing, tissue remodeling and near growing tumors. Under hypoxic conditions tumors secrete VEGF which activates endothelial cells (ECs) in nearby vessels, leading to the migration of ECs out of the vessel and the formation of growing sprouts. Several mechanisms are involved in angiogenic EC migration, such as chemotaxis, haptotaxis, haptokinesis and proteolysis of the extracellular matrix (ECM). In this thesis we present a cell based model of angiogenesis, based on the Cellular Potts Model (CPM), which includes these mechanisms in simple rules. We show that this simple set of rules is sufficient to form sprouts and even branching vascular networks.

Table of Contents

Acknowledgments

First of all I would like to thank Roeland Merks, my supervisor at the CWI, for his guidance, encouragement and support. He gave me the freedom to explore my own ideas, but always kept an eye on the process and the steps to be taken. In times of doubt, his enthusiasm and helpful tips were just what I needed. I thank Jaap Kaandorp, my supervisor at the UvA, for his mentorship the last two years. It was fun being a student again. Finally I would like to thank all colleagues at the CWI for the opportunity to be a full member of their group and to get a taste of scientific life.

Chapter 1

Introduction

1.1 Background

Angiogenesis, the formation of new blood vessels sprouting from existing vessels, is an important process during development, reproduction and tissue repair. However, angiogenesis can also be a pathological process. For example, it is required for tumors to sustain their growth. A lot of research has been done to get more insight in this process, to find the major regulators of angiogenesis and to learn about the mechanisms involved in the initiation, elongation and branching of new blood vessel sprouts. This knowledge could for instance help finding new therapies against cancer [1-3].

1.2 Scope and Objective

In this thesis we will discuss what is known today about angiogenesis, in particular the process of blood vessel formation induced by growing tumors. We will focus on the chemical and mechanical mechanisms that regulate the directional migration and proliferation of endothelial cells, the cells that form a new growing blood vessel sprout.

In particular we are interested in the interactions between endothelial cells and the extracellular matrix. How do cells respond to the composition of the matrix and in what way does this influence the growth and branching of a new sprout? Can these interactions explain characteristics of sprouting angiogenesis?

We developed a cell based model to find answers to these questions. Cell-based models describe cell behaviors, including cell-cell interactions and the interactions of individual cells with their micro-environment, in terms of simple sets of rules. Thus cell-based models can give new insights in the mechanisms which are important for sprout formation and branching [4].

1.3 Organization of rest of thesis

In the following chapter we will give an overview of the processes involved in sprouting angiogenesis. We will focus on the interactions between cells and the extracellular matrix. In chapter 3 we will discuss and compare existing models of angiogenesis. Next we present our cell-based model of angiogenesis and describe the process of translating experimental observations and biological theories into a model. In the final chapters we will present the simulation results, discuss our model and give suggestions for improvements.

Chapter 2

Cell-matrix interactions during angiogenesis

2.1 Hypoxic tumors induce angiogenesis

Small tumors up to a size of ~1 mm can absorb, by simple diffusion, sufficient oxygen and nutrients from their direct environment. When a tumor grows beyond this size tumor cells will lack oxygen and become hypoxic. This turns on the so-called 'angiogenic switch', which leads to an increased expression of several angiogenic factors [5-6].

One of the key angiogenic factors is vascular endothelial growth factor (VEGF). With VEGF we usually mean VEGF-A, which is a member of the VEGF family. VEGF-A has several isoforms, resulting from alternative splicing. A number of these isoforms have a heparin-binding domain and bind to the extracellular matrix (ECM), others are soluble factors [6].

VEGF released by a tumor diffuses into the surrounding tissue, establishing a chemical gradient between the tumor and nearby blood vessels. When it reaches a vessel, it binds to cell surface receptors on endothelial cells (ECs) which form the inner lining of blood vessel walls. This activates the ECs, resulting in increased cell survival, migration and proliferation [7].

ECs activated by VEGF first degrade the basement membrane of the parent vessel and then migrate into the extracellular matrix (ECM) towards the tumor. First, small sprouts are formed by aggregation and migration of ECs that are recruited from the parent vessel. The sprout will further extend when some of the ECs in the sprout wall begin to divide [5, 8]. During this process the vessel sprout will form new branches, and these branches can reconnect again, a process called *anastomosis*. Recently, Fantin and co-workers reported that macrophages can act as 'bridge-cells' in this process, mediating the fusion of the tips of two sprouts [9]. Finally the vascular tree reaches

the tumor, providing it with nutrients and oxygen. Once vascularized, a tumor is more likely to become malignant and to spread and metastasize to other parts of the body [10].

2.1.1 Endothelial cells take on different roles

During angiogenesis ECs can have different phenotypes [11-12]. Cells at the tip of the sprout, *tip cells*, lead the new formed vessel. Their task is to navigate and they actively extend filopodia, which are spiky protrusions, to sense and respond to guidance cues in their environment. They can secrete proteases to degrade the extracellular matrix. Tip cells do not proliferate (grow and divide).

Stalk cells are cells trailing the tip cells. They are less motile and they barely extend filopodia. Stalk cells proliferate when stimulated with VEGF [13] and they deposit ECM components. Their task is to elongating the stalk, to form lumen and connect to the circulation.

Once the vessel has formed, cells turn into the *phalanx* phenotype; they become quiescent and mostly stop dividing. The key function of the vessel is then to supply blood and oxygen to tissues [12].

Tip cell selection and induction is regulated with the endothelial DLL4/NOTCH pathway, which is stimulated by VEGF. This signaling pathway inhibits tip cell formation near other tip cells through lateral inhibition [11].

2.1.2 Proliferation is required to reach the tumor

Sprouting is possible without proliferation of stalk cells. However proliferation is necessary to sustain sprouting for a longer period and to grow a large enough sprout that can reach the tumor. [7, 10]

Although the general idea is that proliferation occurs behind the tip cell, there is no consensus about the exact location of EC mitosis during angiogenesis. Experiments have shown that proliferation can occur some distance behind the sprout tip [10, 14], at the base of a new sprout [10, 15], and even at the tip of the sprout [8, 15-16].

Several studies suggest that proliferation only occurs when the connection between adjacent cells has been disrupted. Therefore it is possible that during angiogenesis mitosis occurs as a result of gaps between ECs in the new sprout [8].

2.1.3 The extracellular matrix has many roles in angiogenesis

The extracellular matrix is a mesh-like network of macromolecules secreted locally by cells. The main components of the ECM are proteoglycans, fibrous proteins such as collagen and elastin and adhesive proteins like laminin and fibronectin. In vertebrates the ECM constitutes the major part of the connective tissue and it forms the basement membrane (or basal lamina), which is a thin sheet of ECM underlying epithelial cells [17].

The ECM has many roles in angiogenesis. It is essential for EC migration, proliferation and survival, since it provides structural support and chemical cues for cell adhesion and motility. ECM components like collagen I and fibrin are capable of supporting chemotactic migration. The density and spatial distribution of ECM proteins such as fibronectin and collagen can affect the speed and direction of cell migration. Furthermore, ECs are able to secrete and degrade ECM components [18].

2.2 Cells migrate by attachment to the ECM

Many studies of cell migration describe in vitro experiments where cells are plated on a dish coated with ECM components. In other experiments, cells are seeded in a three dimensional matrix, in which they show distinct migrating behavior.

The following steps describe how cells move on two-dimensional substrata. First they extend filopodia to sense signals like VEGF gradients in their direct environment. Then sheet-like extensions, called lamellipodia, will form dynamic attachments to the ECM at the front of the cell. Next the stress fibers within the cell contract, which results in a detachment of the rear of the cell. Finally the cytoskeleton relaxes, adhesive and signaling components are recycled and the cell repeats the cycle. [19].

In three-dimensional situations cells behave differently. They have a more elongated and spindle-like shape due to the physical restriction of matrix fibrils. Instead of extending lamellipodia, the cells form pseudopodia following the direction of matrix fibrils. Migrating cells in a 3D matrix have less stress fibers, focal adhesions and spreading. Because the 3D matrix forms a physical barrier around the cells, proteolysis of ECM by cells is necessary for motility [20].

Cells attach to the ECM by reversibly binding transmembrane receptors, mostly integrins, to ECM proteins. The integrin family includes more than 20 members. They bind their extracellular domain to specific ligands such as fibronectin, collagen and laminin and cluster in the membrane to form adhesive contacts called focal adhesions. During EC migration focal adhesions and stress fibers are aligned in the direction of movement resulting in polarized cells [19].

Cell-ECM adhesions regulate cell migration in two ways. They have an adhesive function, binding the extracellular matrix to the actin cytoskeleton, and a signal transduction function, regulating molecules important for cell motility [20].

VEGF can stimulate cell migration in several manners. It increases the expression and activation of several integrins involved in angiogenesis. Cell-cell adhesions inhibit cell migration and need to be broken down to allow cells to migrate. VEGF can break endothelial cell-cell contacts by disrupting the VE-cadherin/β-catenin complex at adherens junctions [19].

2.3 Cell migration is directed by chemotaxis

Chemotaxis is the directional migration of cells in response to gradients of extracellular soluble chemicals. Various cytokines regulate chemotactic migration of ECs, but the three key players are VEGF, bFGF (basic fibroblast growth factor) and angiopoietins [19].

In their study of retinal angiogenesis Gerhardt et al. demonstrated that VEGF independently regulates EC migration of tip cells and proliferation of stalk cells

(Gerhardt, Golding et al. 2003). Their experiments showed that endothelial tip cells extend long filopodia in response to VEGF. These filopodia were guided by a VEGF gradient, resulting in the directed migration of the tip cells (Figure 1). However stalk cell proliferation did depend on the actual concentration of VEGF instead of the gradient. Both functions are mediated by the receptor VEGFR2, but the signals seem to be interpreted differently by the two EC subtypes.

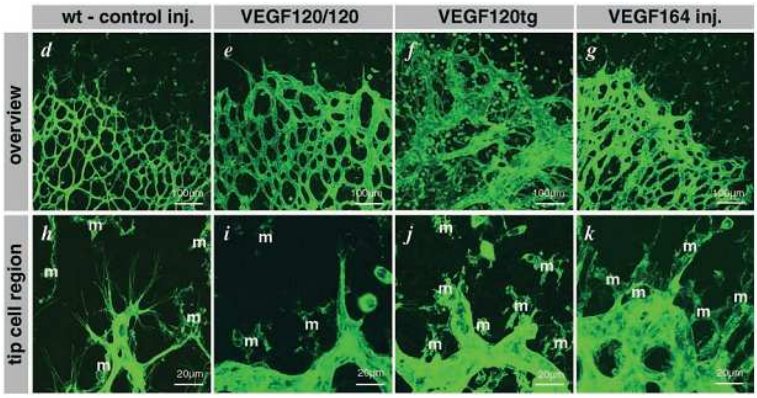

Figure 1 VEGF gradients are necessary for directed tip cell filopodia extension. (From [13]).

Barkefors et al. used a microfluidic chemotaxis chamber (MCC) to study EC migration in response to different VEGF gradients [21]. They observed that a stable gradient of both the isoforms VEGF165 and VEGF121 is sufficient to induce chemotaxis of ECs. Since VEGF121 is unable to interact with several coreceptors, this proved that a stable gradient of VEGF suffices for chemotaxis and interactions between VEGF and coreceptors are not required for a chemotactic response. Furthermore, the authors identified a minimal gradient steepness required for induction of chemotaxis and they showed that chemotaxis is reduced when cells reach the high end of the VEGF gradient. The experiments demonstrated that the shape of the VEGF gradient controls the migratory response of ECs.

2.4 Haptotactic migration can play a role in angiogenesis

The local degradation and deposition of matrix proteins by ECs and the heterogeneity of the extracellular matrix can all create local gradients of ECM components which

can drive endothelial cell migration, a process called *haptotaxis*. Haptotaxis of ECs is mainly triggered by the adhesive interactions between ECM components and integrins [19].

While the role of haptotactic migration in angiogenesis has not yet been established [18], in vitro experiments have shown that collagen [22] and fibronectin [23-24] gradients can guide EC migration, and therefore it is plausible that gradients of these components in vivo may lead to haptotaxis as well.

Senger et al. studied the function of two specific integrins in haptotactic migration of ECs in a gradient of immobilized collagen I [22]. Addition of antibodies against these integrins resulted in a significant reduction of directed migration towards collagen.

Smith et al monitored ECs on substrates with linear gradients or uniform concentrations of fibronectin in a highly controlled environment [23]. The experiments demonstrated that the drift speed of ECs increased on fibronectin gradients compared to uniform substrates. In a subsequent study they measured the response of cells to a range of fibronectin gradient slopes [24]. They showed that the cellular drift speed increased linearly with haptotactic gradient slope.

2.5 Haptokinesis: Cell sensitivity to ECM concentrations

While haptotaxis is the directional migration of cells up ECM gradients, haptokinesis is the sensitivity of cells to absolute concentrations of ECM components. Several experiments demonstrated that cell speed, spreading and membrane activity show a biphasic dependence on ECM concentrations, both on 2D substrates [25-30] as in 3D matrices [31]. We will describe some of these experiments and give possible explanations for the experimental observations. In chapter 4 we will describe our computational single cell experiments with which we tested each of these hypotheses.

2.5.1 Haptokinesis explained with the detachment theory

Palecek et al. measured the mean speed of migrating CHO (Chinese hamster ovary) cells plated on different concentrations of fibronectin and fibrinogen [28]. This speed

was maximal at intermediate ECM ligand concentrations regardless of integrin expression level or integrin-ligand binding affinity. At lower ligand levels cells were more rounded and extended more unstable lamellae that couldn't move the cell body. At high ligand levels cells were very spread and extended lamellae similar to migrating cells, but the cell body didn't move very well.

In another study [27] DiMilla and coworkers showed that the migration behavior of Human Smooth Muscle Cells (HSMCs) on substrates coated with the ECM proteins fibronectin and collagen IV, varied with the concentration of each matrix protein, showing again a biphasic dependence: cell speed and persistence time reached a maximum at intermediate concentrations of both proteins.

Cells migrate at maximum speed at intermediate levels of adhesiveness. The general explanation for this behavior, which we shall call the 'detachment theory', is the idea that at low ECM densities, a cell cannot form strong and stable adhesions at the front to generate a traction force, so no movement is possible and the cell spreads poorly. At high densities a cell cannot detach adhesions from the substrate and therefore the cell will be well spread and immobilized, so again locomotion does not occur. Consequently cells have maximal migration speed at intermediate ECM densities, because then they are able to form new adhesions at the front, and are also able to break attachments at the rear [27-28, 32].

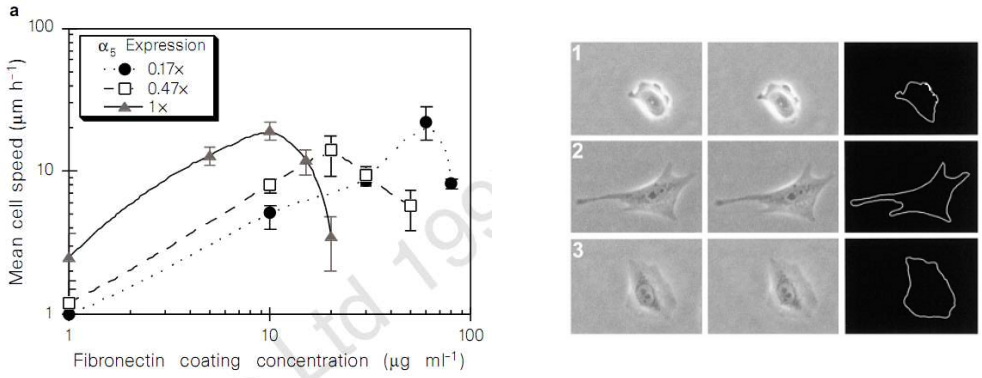

(a) (b)

Figure 2 Maximal (a) cell speed [28] and (b) spreading [29] at intermediate ECM concentrations.

2.5.2 Haptokinesis explained with the receptor saturation model

Although in Palecek's experiments [28] cells were most spread on high ECM densities, Gaudet et al. presented experimental results where both cell spreading and speed were maximal at intermediate collagen surface densities [29]. They measured the projected area, migration speed and traction force at various type I collagen surface densities in a population of fibroblasts. Initially the cell area was an increasing function of surface density, but above a certain concentration the area declined. This threshold collagen density was approximately equal to the cell surface density of integrin molecules.

The 'receptor saturation' model can explain these observations [29]. At low densities, the number of ligands available to a cell is low, and therefore the cell cannot spread effectively. With increasing densities, more integrins can bind to ligands, leading to increased spreading. At the transition point all the integrins on the cell are bound to the substrate. Further spreading is impossible since there are no free integrins available. If the collagen density is increased beyond this point, the saturation of integrin receptors will be possible with a lower level of spreading. So the cell is less spread even though the substrate is more adhesive.

2.5.3 Haptokinesis explained with altered signaling

In the study of Cox et al. cells were plated on different concentrations of fibronectin [26]. The authors reported that membrane activity was maximal at intermediate substratum concentrations. Cell spreading, however, was optimal at high substratum concentrations and lower at intermediate and very high concentrations.

Members of the Rho family play an important role in regulating migration. For that reason Cox and coworkers measured the activity of the genes Cdc42, Rac1 and RhoA in their experiments. The activation of Cdc42 and Rac1 showed a biphasic dependence on fibronectin concentration in line with optimum cell polarization and protrusion. RhoA activity remained elevated at higher substratum concentrations.

Their findings suggest that adhesion-dependent signaling is a mechanism to stop cell migration by regulating cell polarity and protrusion via genes of the Rho family. Cox and coworkers imply with their study another mechanism to explain the haptokinetic observations, which we will refer to as 'altered signaling'.

2.6 Other mechanisms can influence cell migration

Apart from chemotaxis, haptotaxis and haptokinesis, several other mechanisms can regulate the migration of ECs. For example shear stress mechanically influences the response of ECs to haptotactic and chemotactic signals [19]. Aligned fibers in the ECM can guide cell migration (topographic guidance) and these guiding structures can in turn be remodeled by EC tip cells[20]. Differences in ECM rigidity or stiffness can also direct migration, a process called 'durotaxis' [20, 31].

2.7 ECs secrete proteolytic enzymes in order to degrade the ECM

Sprouting endothelial cells must break through their basement membrane and invade into the extracellular matrix in order to form a new capillary. This process requires proteolytic degradation of the ECM [33].

Endothelial tip cells express matrix metalloproteinases (MMPs) that can break down ECM components. MMPs are a family of more then 20 zinc-dependent enzymes.

They can be divided into two structurally different groups, the secreted MMPs and membrane-type MMPs (MT-MMPs). Together the MMPs can degrade all known mammalian extracellular matrix proteins. This includes fibrin, whose breakdown was usually ascribed solely to plasmin, another important proteolytic enzyme [33-34].

Most MMPs -except for the MT-MMPs- are secreted by the cell as latent enzymes. Their activation occurs in the extracellular compartment; MT-MMPs are activated inside the cell. The activity of MMPs is furthermore regulated by tissue inhibitors of metalloproteinases, TIMPs. Cells can localize the proteolysis of extracellular matrix to specific areas of the cell surface, such as the leading tip of a migrating cell, by fine-tuning the interactions with receptors and inhibitors. This increases the efficiency of invasion while preventing the destruction of the required matrix scaffold [33-35].

MT1-MMP is generally considered to be the most important player in pericellular proteolytic activity and is essential in the migration of cells in type I collagen [33, 36-37]. MT1-MMP can degrade many ECM proteins, including collagens, gelatin, and fibronectin. It associates with the plasma membrane, resulting in matrix degradation close to the cell surface. Furthermore it can activate MMP-2 and MMP-13 which amplifies the proteolytic process [33-34].

MMPs, especially MMP-2, MMP-9 and MT1-MMP, appear to be required for angiogenesis. Quiescent ECs produce little or no MMPs, but during wound healing, inflammation and tumor growth MMPs are strongly induced and activated in capillary sprouts [33-34]. Furthermore, several studies have shown that MMP inhibitors could inhibit angiogenesis [34-35]. Activation of proteases can be induced by angiogenic growth factors and inflammatory cytokines. For example MT1-MMP is induced in ECs by several factors, such as VEGF and HGF (hepatocyte growth factor) [33-34].

2.7.1 Other functions of MMPs and their proteolytic products

It was long thought that the only function of MMPs was to degrade ECM components. Recent studies however show that extracellular proteolyses can also regulate endothelial cell function in a more indirect way.

Growth factors bound to ECM components can be released by MMPs. For example, Hawinkels et al. reported that MMP-9 can release matrix-bound VEGF, making it more available to VEGF receptors [38]. Furthermore several angiogenic growth factors like VEGF and TGF-b (transforming growth factor beta) require proteolytic processing to become active [33].

Proteolytic fragments of the ECM and other molecules have been reported to show regulatory activity in angiogenesis, either positive or negative. They are often called 'matrikines' [33].

2.8 Summary

In this chapter we discussed some of the main mechanisms that are involved in tumor induced angiogenesis. One of the key players is VEGF. First of all it activates ECs, promoting their proliferation, survival and migration. Furthermore, the migration of ECs is guided by VEGF gradients between the tumor and the parent vessels. In addition VEGF promotes ECM degradation by stimulating the expression of MMPs.

Angiogenesis depends on highly regulated interactions between cells and the extracellular matrix. In order to invade the ECM, cells need to break down ECM components, but cell-ECM adhesions are required for cell motility. Cell speed and migration direction is influenced by concentrations and gradients of ECM densities.

To what extent play chemotaxis, haptotaxis, haptokinesis and proteolysis a role in sprouting angiogenesis? Are they sufficient mechanisms for the growth of new vessel sprouts and the formation of branching vascular structures? Mathematical models of angiogenesis can be a means to answer these questions. In the next chapter we will discuss several existing models of angiogenesis.

Chapter 3

Models of angiogenesis

3.1 The position of modeling in angiogenesis research

Mathematical models of angiogenesis can offer insight into the processes driving angiogenesis, and test or propose new hypotheses. Many models have been developed of angiogenesis over the last 30 years [39]. This was enabled by the boost in available biological data on this topic and the increasing computational capabilities.

Since tumor angiogenesis is a complex process, the models to date only address a part of the aspects involved in angiogenesis. By focusing on specific mechanisms that can influence the formation of capillary sprouts, these models can help to find the necessary conditions that are required for angiogenesis, such as cell proliferation, haptotaxis, haptokinesis or chemotaxis.

A model is of most value if it is able to reproduce experimental observed phenomena, without explicitly prescribing such events. Such a model should be able to produce emergent behavior from lower level rules. For example, many models of sprouting angiogenesis use high-level rules for branching. We will discuss some of them in the next section. In these models branching is not an emerging phenomenon, but a prescribed event.

In this chapter we will discuss three model categories: continuum models, discrete models and hybrid models (Figure 3). We will describe examples of each category and discuss the advantages and disadvantages of these types of models. We will focus on how cell-ECM interactions are incorporated and whether and how branching occurs in these models.

The Cellular Potts model (CPM) is a cell based framework frequently used to model all kinds of biological phenomena. We will conclude this chapter with a short

description of the CPM and a review of a number of models of angiogenesis based on the CPM.

3.2 Continuum models

Continuum models represent new blood vessels in terms of cell densities, using partial differential equations (PDEs) to describe the average migration and proliferation of cell populations. In these models areas with high densities are blood vessels. Several models make a distinction between the tip and the stalk of a sprout, assuming that tip cells guide the sprout which is formed just behind it.

Although continuum models can provide valuable insight into aspects of angiogenesis, the disadvantage of these models is their use of cell densities and PDEs. This assumes a large amount of cells to be involved in the process, whereas sprouting angiogenesis concerns a limited number of endothelial cells. As a result continuous models cannot take individual cell interactions and behaviors into account. In addition, these models are not able to predict the actual tree-like vascular structure, because they do not distinct separate sprouts.

3.2.1 A study of chemotaxis and haptotaxis in angiogenesis

The two-dimensional continuum model of Anderson and Chaplain [40] uses PDEs to describe EC, tumor angiogenic factor (TAF) and fibronectin densities. EC migration at the tip of a sprout is influenced by three factors: random motility, (saturated) chemotaxis towards TAF and haptotaxis towards fibronectin. In this model cells do not proliferate. The model incorporates uptake of TAF and fibronectin by ECs.

An important result from simulations was that for the outgrowth of the capillary network a sufficient strong chemotactic response was essential. The interactions between ECs and the ECM were important as well. The uptake of fibronectin and TAF created local gradients that allowed for lateral movement. Without this haptotactic response, cells migrated directly to the tumor.

The model contradicts experimental observations on two points: the speed of the vascular front decreases when approaching the tumor, while in reality the speed increases [39]. Second, although the model has not included proliferation, it produces vessels that in some cases reach the tumor, which disagrees with experimental observations as well [10].

Furthermore, this model is not able to capture relevant processes that happen on a smaller scale, such as sprout branching. Therefore the continuum model was converted to a discrete model, applicable at the level of a single cell. This model will be discussed in the next section where we describe discrete models.

3.2.2 Modeling the onset of angiogenesis

Levine et al. [41] presented a one-dimensional continuum model that describes the onset of angiogenesis. It concentrates on the first phase of neovascularization, namely the changes within the existing vessel. The model tries to predict the site of sprout formation.

In the model EC migration is considered to be a diffusive process which can be modeled with a PDE describing reinforced random walks where transition probabilities are dependent on cell concentration, proteolytic enzymes and fibronectin that forms the basal lamina. Michaelis-Menten kinetics describe reactions in which EC receptors are regarded as catalysts for converting TGF (tumor angiogenic growth factors) into proteolytic enzyme, which in turn breaks down fibronectin and destroys the basal lamina. Secretion and uptake of fibronectin by ECs is modeled as well. The model also includes chemotaxis to TGF and haptotaxis to lower concentrations of fibronectin.

Simulations demonstrated that if there was enough angiogenic growth factor supplied to the capillary wall, the basal lamina would break down. Inside the fibronectin opening two aggregated peaks of EC concentration arose, forming the lining of the growing new sprout.

3.2.3 Extending the model with EC migration into the ECM

Levine and coworkers [42] coupled this one-dimensional model of the initiation of angiogenesis to a two-dimensional model that describes the migration of ECs into the ECM towards the tumor, using mostly the same cell behaviors and biochemical kinetics from the earlier model.

In this complex model cells proliferate in the ECM in response to the proteolytic enzyme and this proliferation is localized behind the leading tip of the sprout. The complex structure of the ECM is accounted for using a porosity constant.

The model uses a phenomenological approach where several experimental observations, such as the localization of proliferation and the acceleration of the growing sprout near the tumor, are explicitly included in the model. Therefore these observations cannot be predicted or understood with this model, they can only be accounted for [39].

3.2.4 Mechanochemical forces in blood vessel formation

The model presented by Manoussaki [43] considers both mechanical and chemical interactions during vasculogenesis (the formation of the initial vascualar network during development) and angiogenesis and investigates the effects of these mechanochemical forces on blood vessel formation.

In this model ECs migrate in response to a chemoattractant source. The cells pull on the viscoelastic ECM and migrate by haptotaxis along the resulting ECM stress lines. This results in narrow vessel-like structures. Cell, ECM and chemoattractant densities are described with non-linear PDEs, containing advection, diffusion and reaction terms.

The simulation results suggest that chemotaxis alone is not sufficient for sprout development and that other mechanisms play an important role as well, such as mechanical forces. The model predicts that chemotaxis together with cellular traction can be sufficient for blood vessel formation.

3.3 Discrete models

Discrete models represent cells as single entities that can behave independently and move, grow and divide given certain prescribed rules. With discrete models one can define cell behaviors and interactions with their local environment in order to show how these can yield complex structures. Since a vessel sprout is normally one or a few cells wide and sprout formation involves stochastic mechanisms, cell-based models are better suited to describe the cellular dynamics during angiogenesis than continuum models, which describe sprouts as cell densities using deterministic differential equations.

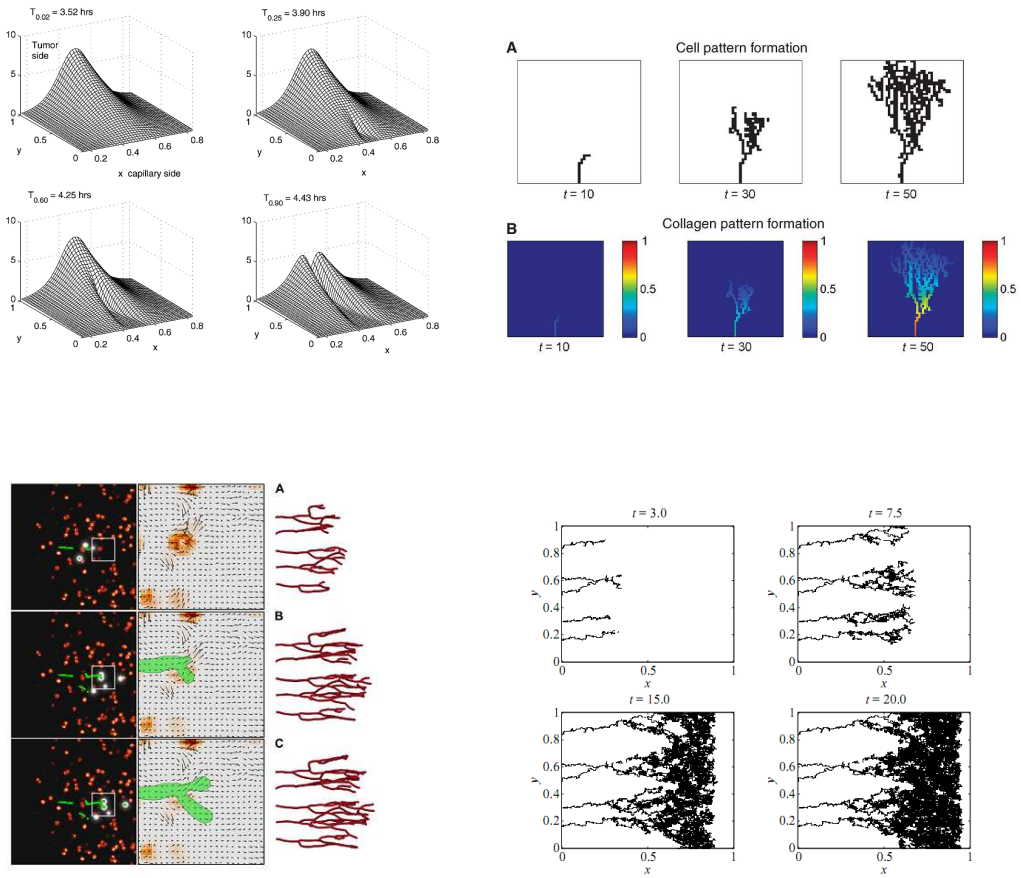

Figure 3 Top row left: continuum model by Levine et al. [42] Top row right: discrete model by Yin et al. [44] Bottom row left: hybrid model by Milde et al. [45] Bottom row right: discrete model by Anderson and Chaplain. [40]

3.3.1 A lattice free agent based model

Stokes and Lauffenburger were one of the first to use a discrete model to describe angiogenesis [46]. They presented a two dimensional, lattice free, agent based model, where new blood vessel sprouts are defined by the trajectory of a migrating cell at the tip of the sprout. Cells within a sprout proliferate to enable sprout growth. Branching is incorporated with predefined branching probabilities. The migration of the tip cells is described by a stochastic ordinary differential equation, which includes chemotaxis and random motion. The model furthermore incorporates anastomosis and branching.

The model investigates how EC motility characteristics like speed and persistence time and chemotactic responsiveness affect the growth rate and structure of the resulting network. The parameters describing random motility, chemotaxis and proliferation were obtained as much as possible from experimental observations of EC behaviors to preserve the predictive value of the model. However the budding and branching probabilities were estimated from experiments on angiogenesis, so these parameters are partly responsible for the ability to predict for example the average vessel lengths in the model.

Simulations demonstrated that the migration rate of ECs mainly determined the rate of vessel outgrowth and that a directional movement, in this model provided by chemotaxis, was required for directed network growth.

3.3.2 Discretizing the continuum model

By discretizing the PDEs in their continuum model and translating them into movement probabilities, Anderson and Chaplain derived a discrete biased random walk model of angiogenesis [40].

The model is based on the assumption that an endothelial cell at the tip of the sprout determines the motion of the whole sprout. In addition sprout branching, anastomosis and cell proliferation were incorporated in this model. The generation of new sprouts occurs at existing sprout tips and only when certain conditions on the

sprout age, EC density and available space are met. The probability that a branch is formed is dependent on the local TAF concentration. Proliferation is added to the model by allowing division of cells at the sprout tip when they are above a certain age.

The results from simulations were similar to those from the continuum model, only now realistic networks were formed. Again, without haptotaxis, the sprout grows faster and there is less lateral movement and therefore less branching. The results confirm those from the continuum model that both chemotaxis and haptotaxis are necessary for the formation of vascular networks in tumor induced angiogenesis.

The discrete model was able to reproduce realistic networks structures. It did reproduce anastomosis, the dendritic structure of the capillary network and the formation of the 'brush border', the increased branching density near the tumor [39].

3.3.3 Migration following collagen cues

Yin and coworkers [44] used a novel microfluid device to study and quantify the behavior of individual cells in well-defined conditions. With these experiments they showed that on a single cell or cell-cell basis, cell migration speed and migration patterns are affected by secreted ECM components and VEGF. From these observations they extracted a set of rules and built a simple agent based model in order to investigate whether these rules are sufficient to reproduce branching patterns in angiogenesis.

In this model ECs are represented by sites on a lattice and they secrete ECM components like collagen which serve as guidance cues for other cells. The cell speed is related to absolute concentrations of collagen with maximal speeds at intermediate concentrations. Cells respond to absolute concentrations of VEGF by progressively loosing their sensitivity to ECM (probably due to increasing ECM degradation). Furthermore ECs move chemotactically to higher VEGF concentrations. Cells can proliferate if they have only one neighbor.

Simulations were able to produce patterns resembling growing and progressively branching vessel sprouts. Yin and colleagues showed that no specific rules on branching and no heterogeneous ECM densities were required to form vascular branching patterns

3.4 Hybrid models

Hybrid models combine continuum and discrete models to represent endothelial cells and other components that play a role in angiogenesis.

In the deterministic 3D model of Milde and co-workers [45] stalk cells and molecular species (VEGF, MMPs and fibronectin) are described as densities whereas tip cells are represented as particles in a discrete, agent based model.

The tip cells secrete MMPs and fibronectin and they bind VEGF. The model incorporates both soluble and matrix-bound VEGF isoforms; the latter are cleaved by MMPs. Tip cells migrate through the ECM, directed by chemotactic and haptotactic cues given by VEGF and fibronectin gradients. They define the morphology of the growing sprout.

EC migration and branching is also influenced by the heterogeneity of the ECM, which is represented by randomly distributed fibers. In addition the fibers in the ECM act as binding sites to fibronectin and matrix bound VEGF. Branching occurs in this model in response to diverging migration directions given by the ECM fiber orientations and the VEGF and fibronectin gradients. Simulations demonstrated that the number of branches depended on the matrix structure and the level of matrix-bound VEGF isoforms.

3.5 The Cellular Potts Model

The Cellular Potts Model (CPM), also known as the Glazier-Graner-Hogeweg (GGH) model, is a lattice based framework, which has frequently been used to model a broad variety of biological phenomena [47-50]. It was developed by Glazier and Graner and represents cell dynamics, like interactions between cells and changes in shape, in terms

of a generalized energy [50]. It finds the lowest energy of a system using a Monte Carlo simulation technique with Metropolis dynamics.

The CPM has many advantages over other cell-based models. It is a simple model, which is easy to extend. The irregular stochastic cell membrane dynamics, like extensions and retractions of protrusions, are explicitly represented, which allows simulating cell interactions with their environment and mimicking the exploratory behavior of cells.

3.5.1 CPM models of angiogenesis

The CPM is used in several simulations of tumor induced angiogenesis. We will discuss four of them below (Figure 4), focusing on the objective of each study, the rules which where incorporated in the models to describe EC behavior during angiogenesis and some of the results.

In their model of tumor-induced angiogenesis Bauer et al. [51] explicitly modeled the heterogeneous composition of the extracellular matrix. They defined endothelial cells, matrix fibers, interstitial fluid and tissue specific cells in the CPM, each having different adhesion energies and different elasticity's. Haptotaxis is naturally incorporated through these adhesion terms, making cell-matrix bonds more favorable over cell-fluid bonds. In their model cells get activated by VEGF and become either tip cells that degrade the matrix and migrate chemotactically up VEGF gradients or stalk cells that grow and divide. Their simulations show that the model is able to reproduce realistic sprout morphologies. They show that inhomogeneities in the ECM can be a mechanism for branching. Furthermore their simulations show that steep VEGF gradients result in narrow sprouts and shallow gradients in more swollen sprouts, which is consistent with empirical observations [13].

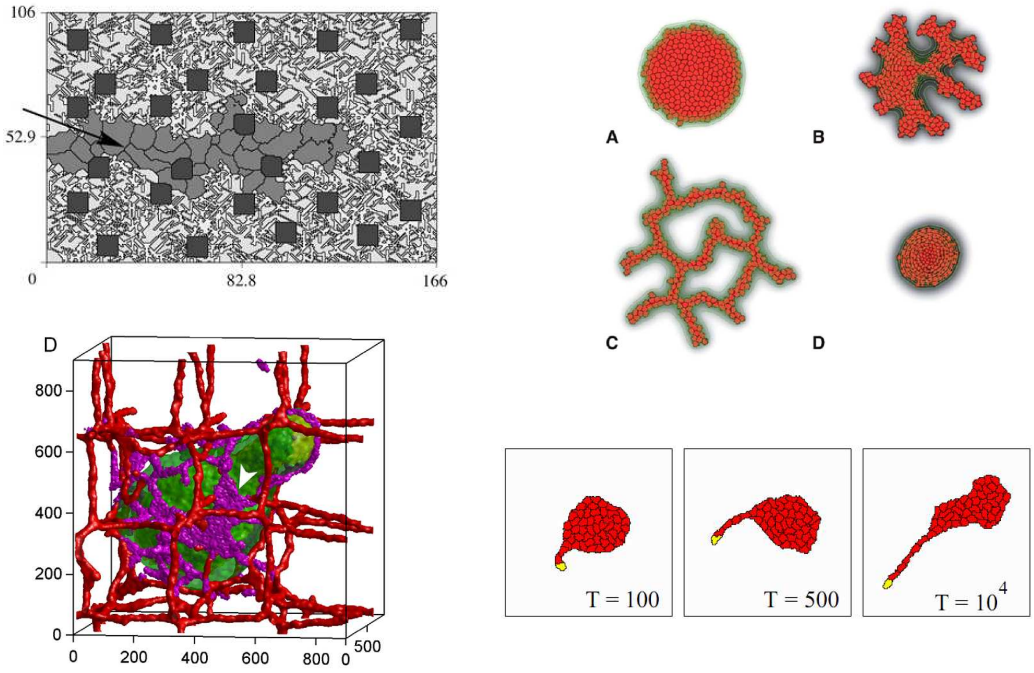

Figure 4 CPM models of angiogenesis. Top row left: Bauer et al. [51] Top row right: Merks et al. [52] Bottow row left: Shirinifard et al. [53] Bottom row right: Szabo et al. [54]

Merks et al. [52] developed a CPM model to investigate if ECs autonomously organize into vascular patters without prepatterns of morphogens. Furthermore, they asked whether vasculogenesis and angiogenesis are regulated by the same mechanisms, signals and cell behavior. In their model cells secrete a chemoattractant, which attracts surrounding cells. From experiments it is shown that chemotaxis is inhibited at cell-cell surfaces (contact inhibition) [55]. Therefore the CPM was extended with the rule that only in the case of extension or retraction at cell-ECM surfaces the chemotactic energy will be included in the calculation of the energy. Two scenarios were tested: one where cells both extent and retract along chemotactic gradients and one where retractions are chemotactically neutral. In either cases, both sprouting-angiogenesis and vasculogenesis occurred, but in the latter case higher intrinsic cell motilities were needed. Their results suggest that sprouting in aggregates of cells secreting a chemoattractant can occur because (at low cell motilities) the branching resembles a 'buckling instability' and (at high motilities) more shallow

gradients at protrusions make it more likely for cells to extend outward-directed pseudopods.

Shirinifard et al [53] presented a 3D CPM model of tumor growth and tumor induced angiogenesis. The model focuses on the growth of a tumor in response to the supply of oxygen. Goal of their simulations was to get more insight in differences in tumor growth with our without angiogenesis. In the model ECs are also activated when VEGF concentrations exceed a certain threshold. Activated cells proliferate and chemotax up a VEGF gradient. The model incorporates contact-inhibited growth of neovascular cells. When the common surface area with other neovascular cells is less than a threshold, the cell grows, with a growth rate related to the VEGF concentration. The cells divide if their volume reaches a certain doubling volume. To self-organize the ECs into capillary-like networks, the model was extended with autocrine chemotaxis to a very short-diffusing chemoattractant, as described in [48]. The model neglects proteolytic activity of ECs.

Szabo et al. [54] argued that during sprout formation stalk cells cannot be totally passive. If cell-cell adhesion is analogue to surface tension, then tip cells are not able to 'pull' the sprout forwards, because of the Plateau-Rayleigh instability. (Just like a falling stream of fluid breaks up into smaller packets with the same volume but less surface area.) Therefore the authors suggested that stalk cells move autonomously as well. They show with CPM simulations that cell-cell adhesion is insufficient to maintain cell supply to expanding sprouts; cells in sprouts have more cell-matrix boundaries than cells at the surface of an aggregate of cells which results in an increase in energy. They extended the CPM with leader cells, preferential attachment to elongated cells and cell polarity. Simulations yielded sprouting dynamics comparable to experimental observations.

3.6 Summary

Many models of angiogenesis have been developed to get more insight in the mechanisms involved in this process. In this chapter we discussed continuum, discrete

and hybrid models. We argued that cell based models are the best choice for modeling angiogenesis, since angiogenic sprouting involves only a few cells and we therefore need to able to define rules on the level of an individual cell. In particular, the CPM can be a good basis for this goal, since it explicitly models the irregularities in cell shape and behavior.

Each of the discussed CPM models used different sets of rules on the level of individual cells to model sprout formation during angiogenesis. This shows that different mechanisms, such as matrix inhomogeneity, chemotaxis to autocrines, contact inhibition of chemotaxis, cell polarity, and preferential adhesion to elongated cells can all play a role in the formation of vascular patterns.

In the next chapter we will present our model of tumor induced angiogenesis, where we focus on the interactions between ECs and the ECM. It is based on the CPM and extended with these cell-matrix interactions.

Chapter 4

A cell based model of ECM-guided EC migration during angiogenesis

Our model defines cell-matrix interactions on the level of individual cells to study the emerging complex organizations on tissue level. These interactions are chemotaxis, haptotaxis, haptokinesis and proteolysis. Simulations should be able to answer questions like: do these interactions suffice to reproduce aspects of sprouting angiogenesis? Do they provide sufficient explanation for the formation of branching vascular structures?

Our model is based on the following rules: (1) Tumors secrete VEGF resulting in a VEGF gradient. (2) VEGF induces the secretion of MMPs by endothelial cells. (3) MMPs degrade ECM components near the cell surface. (4) Cells move along VEGF gradients and they (5) migrate towards higher ECM densities. (6) Cells speed and spreading are maximal at intermediate ECM densities and (7) cells proliferate if a large part of their surface is in contact with the ECM.

We used a two dimensional Cellular Potts Model (CPM) to implement these rules, we therefore start with a detailed description of the CPM in the following section. Next we will describe how we incorporated our model into the CPM. We give a detailed survey of ways to model haptokinesis and their implementation in the CPM

4.1 CPM explained in more detail

In the Cellular Potts Model biological cells are represented as patches of lattice sites. Each cell has a unique index σ, which is assigned to every lattice site that is occupied by that cell. Furthermore the type of a cell σ is denoted with $\tau(\sigma)$. The extracellular matrix consists of all lattice sites not occupied by cells and is labeled with index $\sigma=0$ and type $\tau=0$.

The interfaces between neighboring lattice sites with unequal index $\sigma_{\mathbf{x}} \neq \sigma_{\mathbf{x'}}$ represent membrane bonds and have a cell-type dependent adhesion energy given by $J_{\tau(\sigma_{\mathbf{x}}),\tau(\sigma_{\mathbf{x'}})}$ (Figure 5).

An area constraint penalizes cell shapes deviating too much from their preferred area. To mimic cell elongation a length constraint is added [48]. The ECM has no area or length constraint.

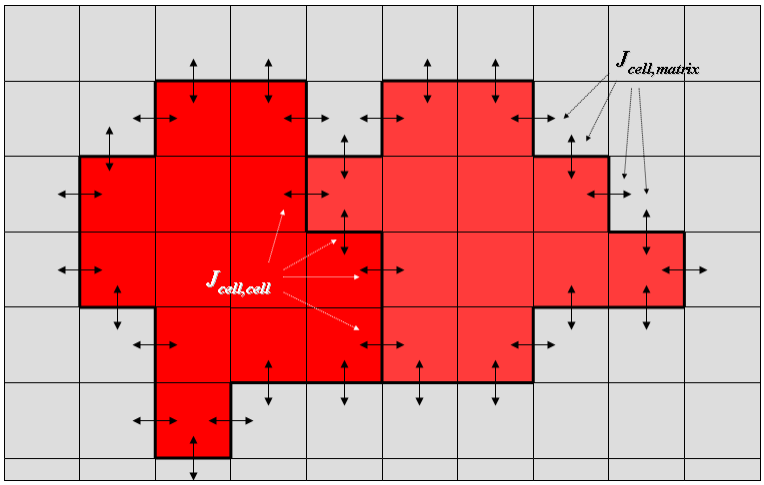

Figure 5 Adhesion energies at cell-cell and cell-matrix interfaces.

The 'effective energy' is given with the CPM Hamiltonian:

$$H = \sum_{\mathbf{x},\mathbf{x'}} J_{\tau(\sigma_{\mathbf{x}}),\tau(\sigma_{\mathbf{x'}})}(1-\delta_{\sigma_{\mathbf{x}},\sigma_{\mathbf{x'}}}) + \lambda \sum_{\sigma}(a_\sigma - A_\sigma)^2 + \lambda' \sum_{\sigma}(l_\sigma - L_\sigma)^2 \qquad (4.1)$$

where **x** and **x'** are neighboring lattice sites; $\delta_{x,y} = \{1\ ,\ x=y;\ 0,\ x\neq y\}$; a_σ is the current area of cell σ, A_σ its target area and λ the inelasticity; l_σ represents the current length of cell σ, L_σ its target length and λ' the strength of the length constraint.

To mimic membrane extensions and retractions, we repeatedly attempt to replace the index σ of a random lattice site **x** by one of its random neighboring sites **x'**.

We calculate ΔH, the change in total effective energy if we performed the copy and accept the attempt with Boltzmann probability:

$$P(\Delta H) = \begin{cases} 1 & , \text{if } \Delta H < 0 \\ e^{-\Delta H / T} & , \text{if } \Delta H \geq 0 \end{cases} \tag{4.2}$$

where T corresponds to the intrinsic motility of the cells. By accepting energetically unfavorable moves, we prevent the system from getting trapped in local energy minima.

Chemotaxis can be incorporated by including an extra reduction in energy for extensions and retractions towards higher concentrations of a chemoattractant (as described in [49]):

$$\Delta H_{chemotaxis} = -\mu(c(\mathbf{x}) - c(\mathbf{x}')) \tag{4.3}$$

where **x** is the site into which neighbor **x'** copies its spin, $c(\mathbf{x})$ is the local concentration of chemoattractant at site **x**, and μ is the strength of the chemotactic response.

4.2 Model setup

Our model domain is a rectangular dish (size 500 μm × 700 μm) in which endothelial cells are placed behind a vessel wall situated at the 'bottom' of the dish. The cells can migrate through a gap in the wall into the ECM towards the 'top' of the dish in the direction of a tumor which we assume to be located beyond the top of the dish (Figure 6). We define only one type of cell, so we do not make a distinction between tip cells and stalk cells.

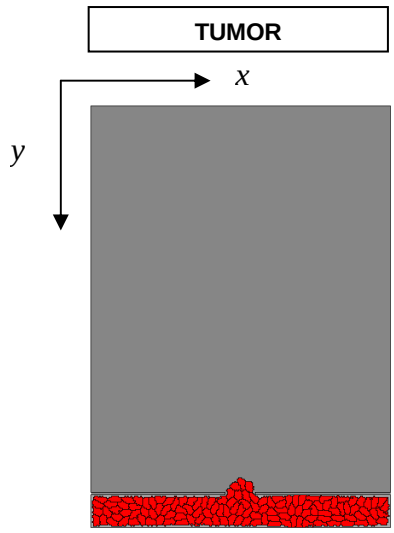

Figure 6 The simulation is initialized with ECs placed behind a vessel wall.

A lattice site represents an area of 2×2 μm. We will set the target area $A_\sigma = 50$ lattice sites corresponding to 200 μm^2 and the target length $L_\sigma = 30$ μm. We set the adhesion energy at cell-cell borders $J_{CC} = 40$ and the cell-matrix energy $J_{CM} = 25$, in order to make attachments between cells slightly favorable over cell-matrix bonds. The intrinsic motility parameter $T = 100$.

When doing a copy attempt we select the source site from the twenty first to fourth nearest neighbors, to improve the isotropy. During a Monte Carlo Step (MCS) we carry out N copy attempts where N is the number of lattice sites. We define a high cell-border energy to prevent cells from adhering to the boundaries of the lattice.

4.3 Modeling VEGF, MMPs and ECM concentrations

We will include three layers in our model that describe the concentration of VEGF, MMPs and ECM. Since MMPs degrade the matrix components, and VEGF induces the secretion of MMPs, we need to allow crosstalk between these layers. This way we can relate the secretion rate of MMPs to the VEGF concentration, and the decay rate of ECM components to the MMP concentration.

4.3.1 VEGF layer

Since the tumor will be relatively large, we assume a constant linear VEGF gradient with equal concentrations at equal y positions throughout the simulation. Therefore we initialize the VEGF layer at the start of the simulation and do not alter it by diffusion, secretion or degradation at later steps (Figure 7).

Given the diffusion coefficient D and the degradation rate ε of VEGF and the concentration at a starting point c(0), we can calculate the analytical solution of the gradient at steady state [56]. If the gradient is caused by diffusion and linear decay, the 1D solution is:

$$c(y) = c(0)e^{-y/\lambda} \quad \text{with } \lambda = \sqrt{\frac{D}{\varepsilon}} \tag{4.4}$$

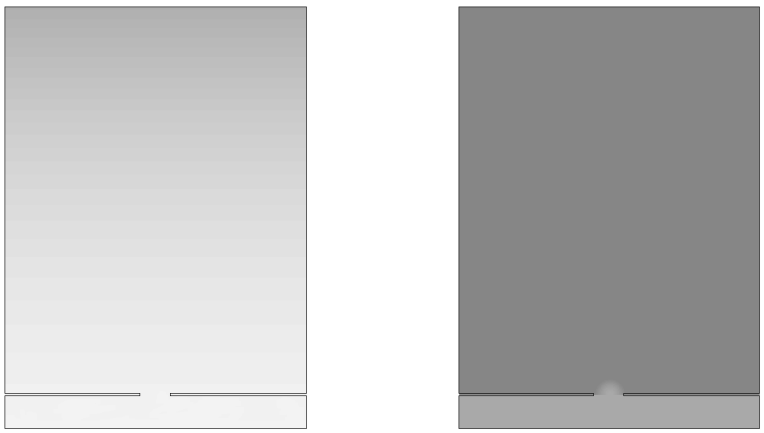

(a) (b)

Figure 7 The constant VEGF gradient (a) and initial ECM density (b).

4.3.2 MMP layer

We will describe the secretion, decay and diffusion of MMPs with a PDE model:

$$\frac{\partial c_M(\mathbf{x},t)}{\partial t} = \alpha_{M\_V} c_V(\mathbf{x},t)(1-\delta_{\sigma_x,0}) - \delta_{\sigma_x,0}\varepsilon_M c_M(\mathbf{x},t) + D_M \nabla^2 c_M(\mathbf{x},t) \quad (4.5)$$

where $c_M(\mathbf{x},t)$ and $c_V(\mathbf{x},t)$ represent the concentration of MMPs and VEGF respectively at site $\mathbf{x}$ at time t ; α_{M_V}, ε_M and D_M are the secretion rate, decay rate and diffusion coefficient of MMP. Again, $\delta_{x,y} = \{1 , x=y; 0, x\neq y\}$, so secretion only occurs at lattice sites occupied by cells and degradation only occurs at ECM sites.

4.3.3 ECM layer

We initialize the ECM layer at the start of the simulation with a high uniform concentration outside the parent vessel, an intermediate concentration inside the vessel and a half circular gradient behind the gap (Figure 7). We assume that ECM components do not diffuse and that the decay rate solely depends on the concentration of MMPs:

$$\frac{\partial c_E(\mathbf{x},t)}{\partial t} = \alpha_E(1-\delta_{\sigma_x,0}) - \delta_{\sigma_x,0}\varepsilon_{E\_M} c_M(\mathbf{x},t) c_E(\mathbf{x},t) \quad (4.6)$$

where $c_E(\mathbf{x},t)$ and $c_M(\mathbf{x},t)$ represent the concentration of ECM and MMPs respectively at site $\mathbf{x}$ at time t ; α_E, ε_{E_M} are the secretion rate and decay rate of the ECM components.

Since in our model degradation only happens at ECM sites, the non-diffusible ECM components will not decay at lattice sites that are occupied by the cells of a growing sprout. Therefore we set the secretion rate $\alpha_E = 0$, creating an ECM concentration at cell sites being the net result of balanced secretion and decay.

We did try an alternative solution by allowing degradation at cell sites and adding secretion of ECM components. However, to avoid a fast accumulation or decay of ECM components the secretion and decay rates needed to be well-tuned, resulting in a model that was very sensitive to both these parameters.

We solve the two PDEs numerically with a finite difference scheme on a similar lattice as the one used in the CPM with $\Delta x = 2$ μm. We set $\Delta t = 2$ seconds and run 15 'diffusion steps' between subsequent MCS. We use fixed boundary conditions. To avoid instabilities we first check whether the combination of Δt, Δx and diffusion coefficient is small enough (Von Neumann stability analysis) to solve with a fast Forward Euler method. If not, we switch automatically to a Crank-Nicolson (CN) scheme. The CN method takes the 'average' of the explicit Forward Euler method and the implicit Backward Euler method, resulting in an accurate and unconditionally stable solution [57].

The VEGF, MMP and ECM concentrations are dimensionless and all have values between 0 and 1. As a consequence the secretion of MMPs will be suppressed as soon as local MMP concentrations exceed the maximum concentration, this agrees with the inhibition of proteolysis by TIMPS.

4.4 Modeling chemotaxis and haptotaxis

Since primarily the extending filopodia of (tip) cells are able to sense and react on chemotactic cues, we consider only extensions of cells into the ECM to contribute to the chemotaxis energy term.

The energy change due to chemotaxis then becomes:

$$\Delta H_{chemotaxis} = -\delta_{\sigma_{\mathbf{x}},0}(1-\delta_{\sigma_{\mathbf{x}'},0})\cdot\mu(c_V(\mathbf{x})-c_V(\mathbf{x}')) \qquad (4.7)$$

where **x** is the site into which neighbor **x'** copies its spin, $c_V(\mathbf{x})$ is the local concentration of VEGF at site **x**, and μ is the strength of the chemotactic response.

This corresponds to incorporating contact inhibition of chemotaxis, reflecting VE-cadherins suppression of pseudopods, and extension-only chemotaxis as described in [52].

In a similar way we implement haptotaxis, the migration towards higher ECM densities. One modification was made however: it would not be realistic for cells to move towards very high densities; therefore we include haptotactic saturation that ensures this restriction:

$$\Delta H_{haptotaxis} = -\delta_{\sigma_{\mathbf{x}},0}(1-\delta_{\sigma_{\mathbf{x}'},0})\cdot\tau\left(\frac{c_E(\mathbf{x})}{1+s\cdot c_E(\mathbf{x})}-\frac{c_E(\mathbf{x}')}{1+s\cdot c_E(\mathbf{x}')}\right) \tag{4.8}$$

Here $c_E(\mathbf{x})$ is the local ECM density at site $\mathbf{x}$, τ is the strength of the haptotactic response and s is a saturation factor.

Note that we consider concentrations of ECM components to be present at or below all lattice sites, so at cell sites as well, since cells are placed in the matrix and we consider a matrix to be present below the cell as well.

4.5 Modeling Haptokinesis

In chapter 2 we have described the detachment theory, the receptor saturation model and altered signaling to explain why cells have maximal speed, spreading and membrane activity at intermediate ECM densities. We translated each of these explanations to a model that could be incorporated into the CPM. We next ran simulations with a single cell placed in an *in silico* dish (size 400 μm x 400 μm) in a uniform ECM concentration to measure the average cell speed and area for a broad range of ECM densities. An acceptable solution should have both optimal speed and area (as measure of spreading) at intermediate ECM concentrations.

4.5.1 Detachment theory in the CPM

The detachment theory states that with a low concentration of ECM molecules there will be not enough adhesive forces for the cell to adhere to the matrix. On the other hand with high ECM densities the adhesions will be too strong to release and retract the rear end of the cell. We implemented this theory in the CPM by replacing the static adhesion energies defined for cell – matrix surfaces (J_{CM} values) by variable adhesion energies. We define higher J_{CM} values for surfaces with low ECM

concentrations and higher J_{CM} values for surfaces with high concentrations at a matrix site (Figure 8):

$$J_{x,y}(c) = \begin{cases} J_{x,y} \cdot \dfrac{c - \varphi \cdot c_{\max}}{c_{\mathrm{mid}} - \varphi \cdot c_{\max}} & \text{if} \quad x = 0 \vee y = 0 \\ J_{x,y} & \text{if} \quad x, y \neq 0 \end{cases} \qquad \text{with } \varphi = 1 + \frac{50}{1+\eta} \tag{4.9}$$

where c is the ECM density at the matrix site, $c_{\max}$ and c_{mid} are the maximum and intermediate ECM density, respectively. The haptokinesis parameter η defines the degree of deviation from the static value, with $J(c_{\max}) \rightarrow 0$ for $\eta \rightarrow \infty$ and $J(c) \approx J_{\mathrm{static}}$ for $\eta = 0$.

The new adhesion energy term now reads:

$$H_{adhesion} = \sum_{x,x'} J_{\tau(\sigma_x),\tau(\sigma_{x'})}(c)(1 - \delta_{\sigma_x,\sigma_{x'}}) \tag{4.10}$$

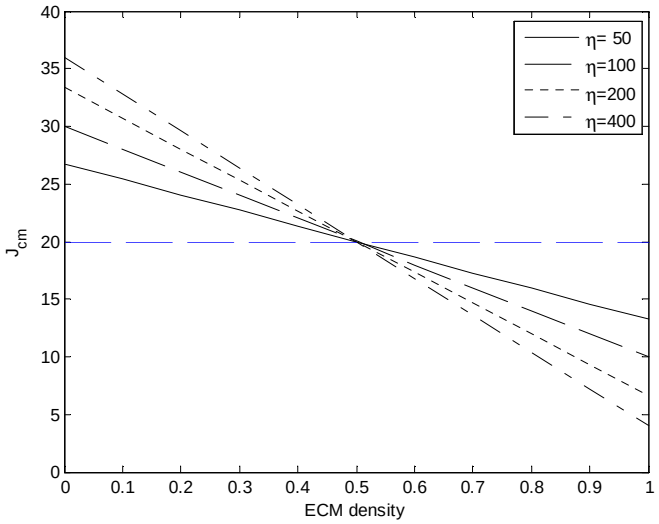

Figure 8 Dynamic adhesion energies J_{CM} as a function of ECM density. The haptokinesis strength η determines the slope or the extent of deviation from the static J_{CM} value.. The horizontal blue line is the static J_{CM} value.

In simulations where one cell was placed in a dish with uniform ECM concentrations we see indeed that this results in a maximal speed at an intermediate ECM concentration, however the area of the cell (which is a measure for spreading) increases with increasing ECM levels (Figure 9).

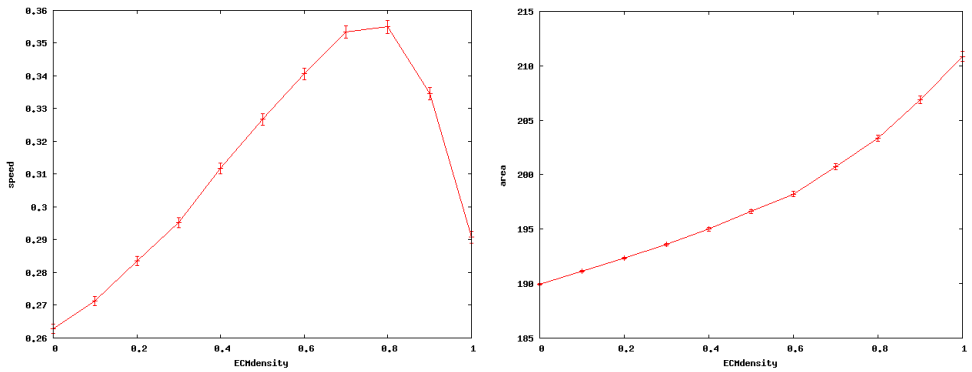

(a) (b)

Figure 9 Testing the detachment model. Average speed (in µm/min) (a) and cell area (in µm) (b) of cells placed in different uniform ECM densities. η = 200. Error bars represent the standard error of the mean (s.e.m.). n = 50.

This can very well be explained by the fact that for high J_{CM} values cells will try to minimize their cell-ECM surface to minimize the energy. With decreasing J_{CM} values, cells will have more affinity to attach to the matrix and will therefore increase their surface resulting in increased spreading. However, in extreme cases, for very low J_{CM} values, the cell looses its integrity, which is another reason not to choose this model (Figure 10).

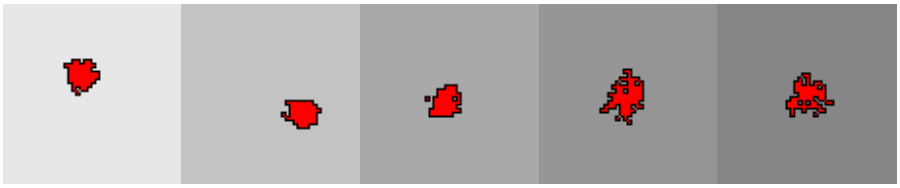

Figure 10 Testing the detachment model. Cell shape is rounded at low densities and irregular at high ECM densities.

4.5.2 Receptor saturation in the CPM

Next we implemented the receptor saturation theory in our model, which states that cells have a limited amount of integrins available to bind to ECM molecules. When the concentration of ECM molecules is low the cell cannot spread optimally. When the concentration is higher, spreading will increase up to a certain threshold level after which the spreading will decrease since all integrins of the cell can make bonds using less cell-matrix surface.

We implemented this theory into the CPM by summing the ECM densities at all lattice sites of a cell. This total concentration is proportional to the matrix molecules that can bind with integrins. We define a maximum number of bonds, which is related to the maximum number of available integrins, the 'saturation threshold'. The number of bonds of a cell is the minimum of this total ECM concentration and the saturation threshold:

$$\text{Bonds}(\sigma) = \min\left(\sum_{\mathbf{x}\in\sigma} c_E(x), \text{Bonds}_{\max}\right) \tag{4.11}$$

Making bonds is considered favorable and therefore we introduce an energy difference term proportional to the difference in number of bonds before and after the copy attempt.

$$\Delta H_{haptokinesis} = -\eta \sum_{\sigma \neq 0} \left(\text{Bonds}(\sigma)_{after} - \text{Bonds}(\sigma)_{before} \right) \quad (4.12)$$

This model did show an optimal spreading at intermediate levels of collagen concentration, but did not result in optimal speed at those levels (Figure 11). On contrary, the speed decreased when spreading was optimal.

However, when we take into account that adding a lattice site to a cell with a large area will have less effect on its center of mass compared to a cell with small area and correct the measured speed by multiplying with the area, we see an increase in speed at intermediate ECM densities Figure 12. However the sudden drop in speed and spreading doesn't agree with experimental results.

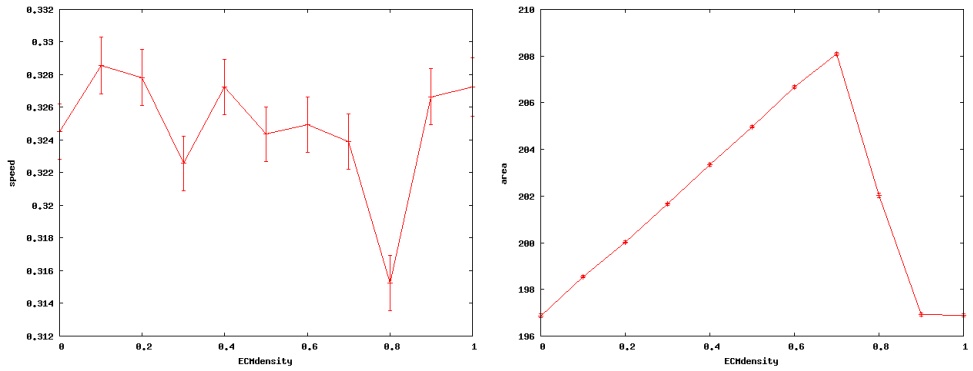

(a) (b)

Figure 11 Testing the receptor saturation model. Average speed (in µm/min) (a) and cell area (in µm) (b) of cells placed in different uniform ECM densities. η = 200. Error bars represent the standard error of the mean.

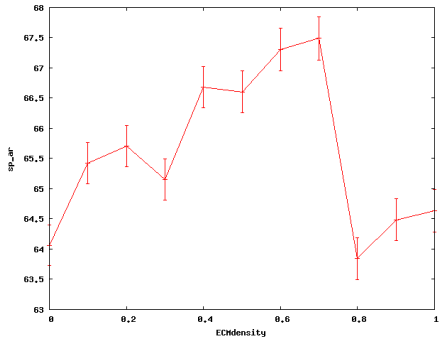

Figure 12 Testing the receptor saturation model. Speed × area as a function of ECM density. η = 200. Error bars represent the s.e.m. n = 50.

4.5.3 Altered signaling in the CPM

Finally we incorporated altered signaling in the CPM. Here the phenomenon of optimal spreading and motility at intermediate levels of ECM density is explained by differences in gene expression in the cell. When ECM concentrations exceed a certain level, cell behavior will change and cells will round up and loose motility. The same can be said for low ECM levels. Experiments have shown that cells will extend most protrusions at intermediate collagen levels.

We integrated this into the CPM in the following way. When cells try to extend into the ECM, the probability of this step is highest at intermediate collagen levels. Intermediate levels will in this case result in an energy decrease, low or high levels will result in an increase in energy. The energy difference caused by haptokinesis is therefore given by the following Gaussian function (Figure 13):

$$\Delta H_{haptokinesis} = -\delta_{\sigma_x,0}(1-\delta_{\sigma_{x'},0})\cdot\eta\left[-1+\frac{0.4}{\rho}e^{\frac{-(c_E(\mathbf{x})-\mu)^2}{2\rho^2}}\right] \qquad (4.13)$$

where μ is the intermediate ECM density, $(c_{max}\text{-}c_{min})/2$ and ρ is set to $(c_{max}\text{-}c_{min})/5$.

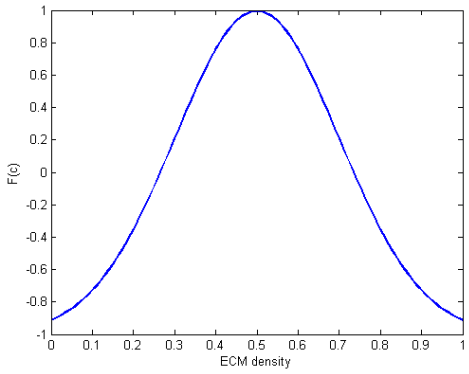

Figure 13 The increase in energy as a function of ECM density.

This results in a bell shaped curve for speed and spreading for low to high collagen concentration levels (Figure 14), which agrees with experimental results [28]. We therefore selected the altered signaling model to describe haptokinesis in the CPM.

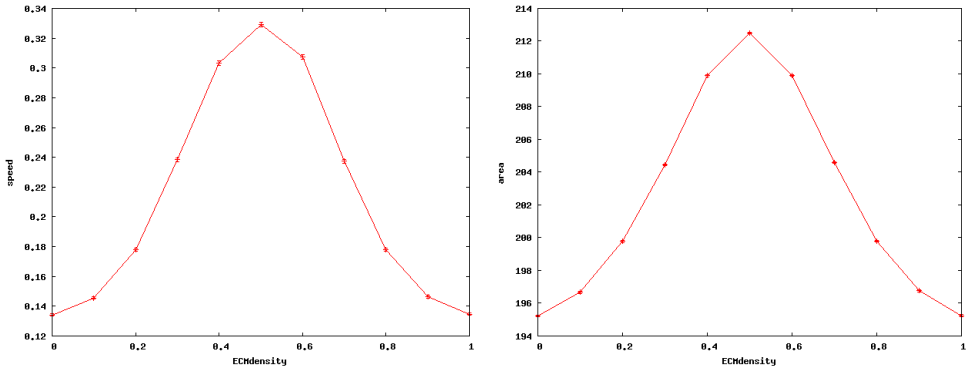

(a) (b)

Figure 14 Testing altered signaling. Average speed (in μm/min) (a) and cell area (in μm) (b) of cells placed in different uniform ECM densities. η = 200. Error bars represent the s.e.m. n = 50.

4.6 Proliferation

During sprouting angiogenesis stalk cells can proliferate. As described in chapter 2, some studies suggest that this only happens just behind the tip cell, while others argue that stalk cells divide at the base of a sprout. The implementation of any of these

options is however complicated. Since VEGF promotes proliferation and following the suggestion that cell division occurs at gaps between ECs [8], we allow proliferation for those cells for which a relatively large part of their surface is in contact with the ECM (and thus in contact with VEGF). The probability of mitosis grows when this proportion increases:

$$P_{\text{proliferation}} = \begin{cases} 0 & \text{, if } \rho < \rho_{\min} \\ \rho - \rho_{\min} & \text{, if } \rho \geq \rho_{\min} \end{cases} \tag{4.14}$$

where ρ is the ratio (cell-ECM surface/total cell surface) and $\rho_{\min}$ is a threshold ratio.

We use Hogeweg's model [58] of cell division by assigning a new index to the grid points on one side of the shortest axis of the dividing cell and giving the daughter cells half the target area and a decreased target length. This polarized division is in agreement with experimental observations of proliferating ECs [59]. By slowly incrementing the target area and target length, cell growth is implemented. In our model we increase the target area of cells every 5 MCS with 2 lattice sites. Furthermore proliferation is only allowed outside the parent vessel, at a minimum distance of one cell length from the vessel wall.

4.7 Summary

Our cell based model of tumor induced sprouting angiogenesis uses the CPM framework to describe the behavior of individual endothelial cells. We added three layers to represent the VEGF, MMP and ECM concentrations and incorporated chemotaxis, haptotaxis, haptokinesis, proteolysis and proliferation as energy difference terms.

The next chapter describes the results of our simulations. We will show that this simple model is able to reproduce realistic vascular sprouts. We use compactness, sprout height and sprout size as quantitative measurements to evaluate the consequences of varying parameters like chemotaxis, haptotaxis and haptokinesis strength or ECM decay rate.

Chapter 5

Results

We ran several simulations with parameter values as described in the previous chapter and as indicated in Table 1. We chose a relatively small diffusion coefficient and high decay rate for MMPs to restrict ECM degradation to the direct environment of the cells. We start with a very high ECM density in the dish, so cells will first need to break down the matrix in order to migrate.

parameter	value	description
μ	5000	chemotaxis strength
τ	300	haptotaxis strength
s	7	saturation haptotaxis
η	200	haptokinesis strength
ε_{E_M}	3e-3	decay rate ECM
α_{M_V}	8e-5	secretion rate MMPs
ε_M	1e-3	decay rate MMPs
D_M	1e-14	diffusion coefficient MMPs
D_V	6e-11	diffusion coefficient VEGF
ε_V	1e-3	decay rate VEGF
$\rho_{\min}$	0.73	threshold ratio for proliferation
λ	25	parameter area constraint
λ'	25	parameter length constraint
ECM density	0.9	initial ECM density outside parent vessel
VEGF concentration	0.05	VEGF concentration at bottom of dish
MCS	40000	number of total MCS

Table 1 Default parameter settings for simulations

Our simulations reproduce vessel sprouts that grow towards the tumor and frequently form branches (Figure 15 and Figure 16). Frequently anastomosis occurs when two

sprouts rejoin (Figure 16 d-g). In some cases branches split off, probably due to a too high pulling force from the leading cells (Figure 16 g-h).

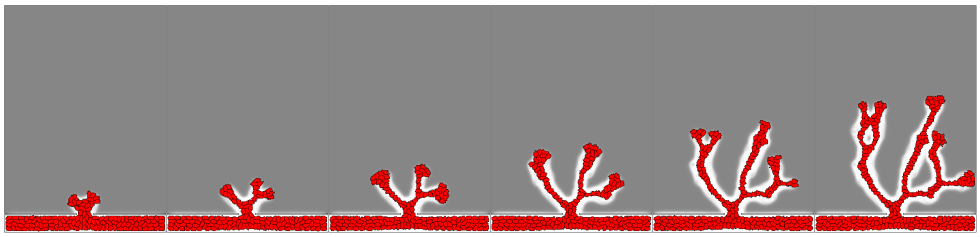

Figure 15 Example of a growing sprout. Subscripts: number of MCS. All parameters as indicated in Table 1.

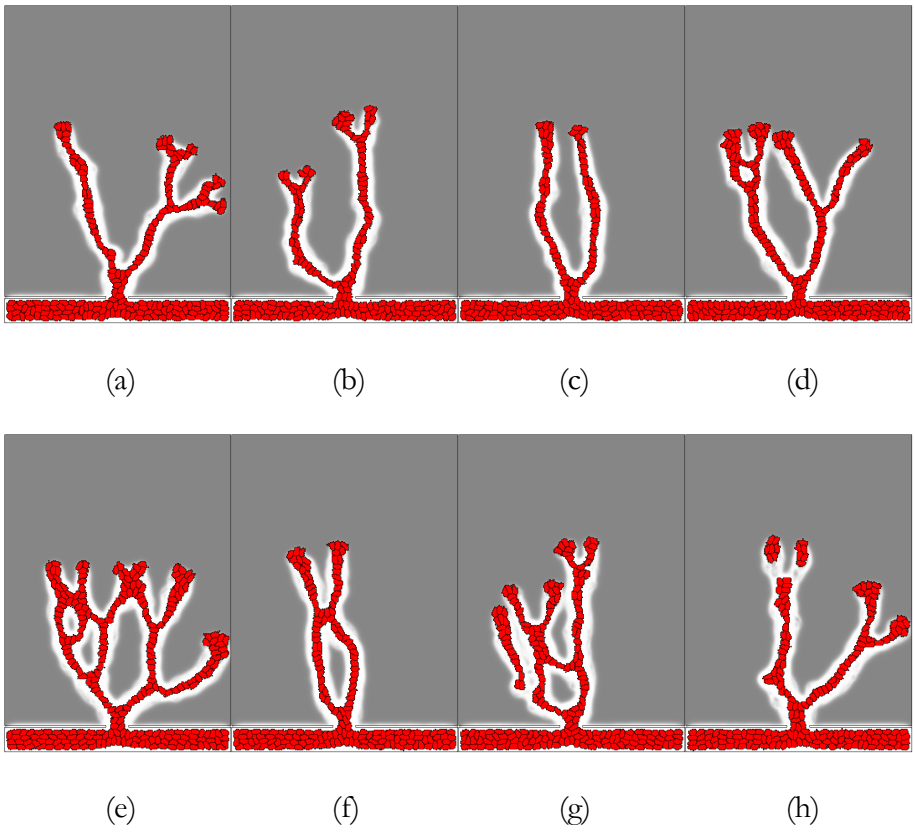

Figure 16 Examples of growing sprouts after 30000 MCSs. All simulations have parameter settings as indicated in Table 1.

5.1 Measuring compactness, height and size of sprout

Although properties like sprout length and size and branching frequency can be evaluated upon visually inspecting the graphical output (pictures and movies) of the simulations, we would prefer to use quantitative measurements that can give us an indication of these properties in order to do a faster and more thorough analysis of the results.

Before doing measurements on the growing sprout, we need to define which cells belong to this sprout. We therefore define the largest 'blob' as the largest set of connected cells and we will consider all cells in this blob that are outside the parent vessel to belong to the sprout. This means that individually migrating cells or branches that have split off are not included in our measurements. We use a fast union-and-find algorithm to determine the largest blob among all cells [60].

We calculate the 'compactness' of the sprout as a measure of branching. We first draw a convex hull around those cells in the largest blob that are located outside the parent vessel. The compactness is the ratio between the total area of these cells and the area of the convex hull [52]. Usually sprouts with high compactness have no or few branches and grow in a direct line towards the tumor. However, extensive branching sprouts can have high compactness as well, since these branches will at the end fill up almost all space.

To measure how fast the new vessel is growing we need to measure the distance of the growing vascular network from the parent vessel. We define the 'height' of the sprout as the largest distance in y direction between any lattice site in the largest blob and the bottom of the dish.

We are also interested in the growth in size of the sprout; we therefore define the 'size' of the sprout as the number of cells of the largest blob. A large size can also be an indication of excessive branching.

5.2 Sensitivity analysis

In order to find out which of the mechanisms of our model plays a key role in sprouting angiogenesis and to study the sensitivity of the model to certain parameter variations we ran simulations where we varied the parameter of interest and kept all other parameters fixed.

5.2.1 Chemotaxis

We first investigated the role of chemotaxis by varying the chemotaxis strength μ. Compactness and the size of the sprout are not sensitive to this parameter, but the sprout grows faster with higher values of μ (Figure 17). This makes sense, as increased chemotaxis will more strongly pull the growing sprout in the direction of the tumor.

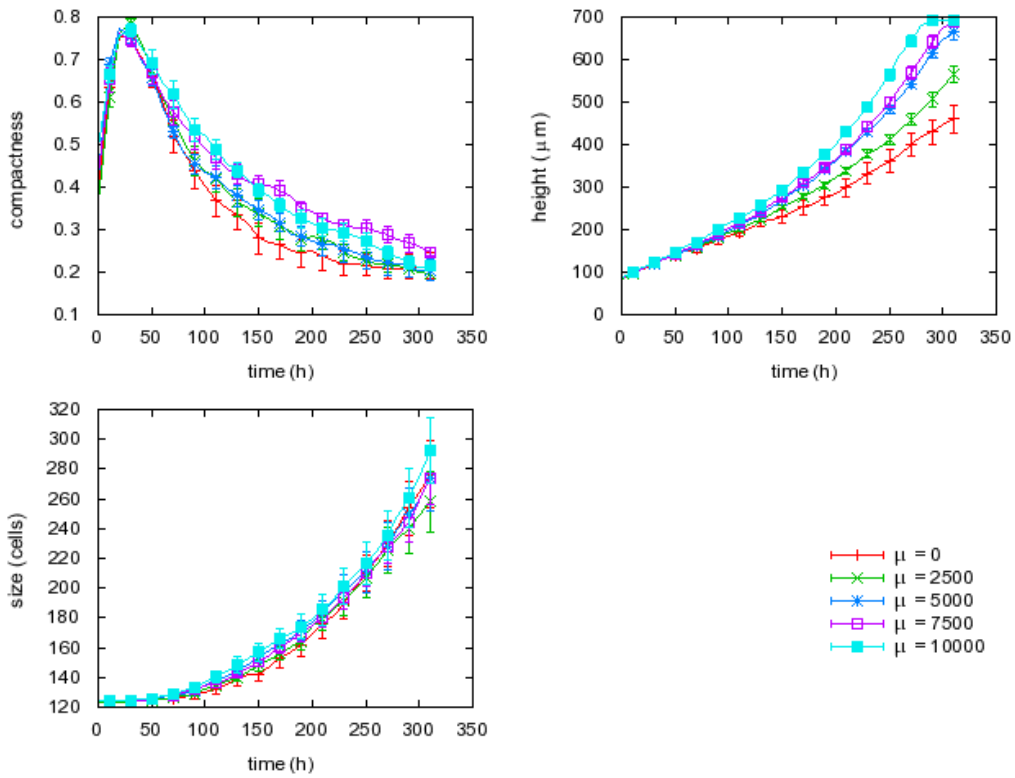

Figure 17 Compactness, height and size of the growing sprout with varying chemotaxis strength. Error bars indicate s.e.m. n = 10.

5.2.2 Haptotaxis

Next we looked at the strength of haptotaxis. While compactness and height show no major differences, the size of the sprout increases with haptotaxis strength (Figure 20), producing more complex, branching networks (Figure 18).

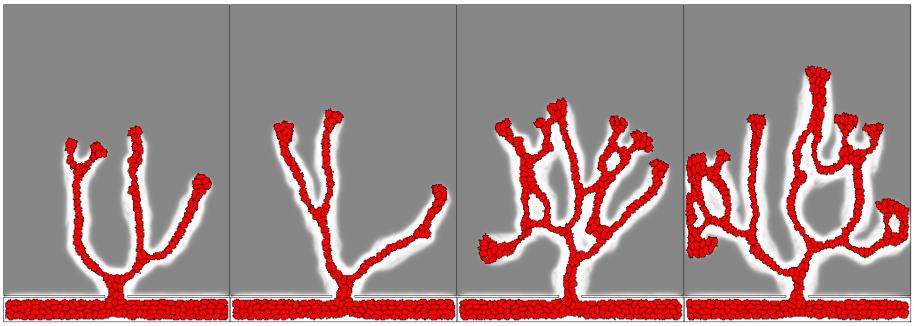

Figure 18 Examples of growing sprouts after 30000 MCSs with different haptotaxis strength (subscripts).

We can explain this as follows. Haptotaxis promotes migration to higher ECM densities, but up to an intermediate ECM concentration. The ECM density near the top of a sprout is higher than in areas at the sides of the sprout tip, therefore haptotaxis can stimulate lateral movement of (cells at) the sprout tip (Figure 19) and this can induce branching.

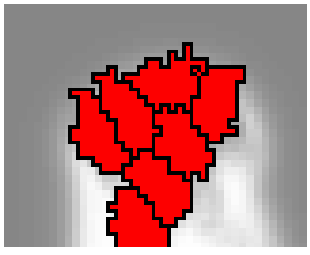

Figure 19 Lower ECM densities at the sides of the sprout compared to the top. Haptotaxis to those densities can promote lateral movement of the sprout.

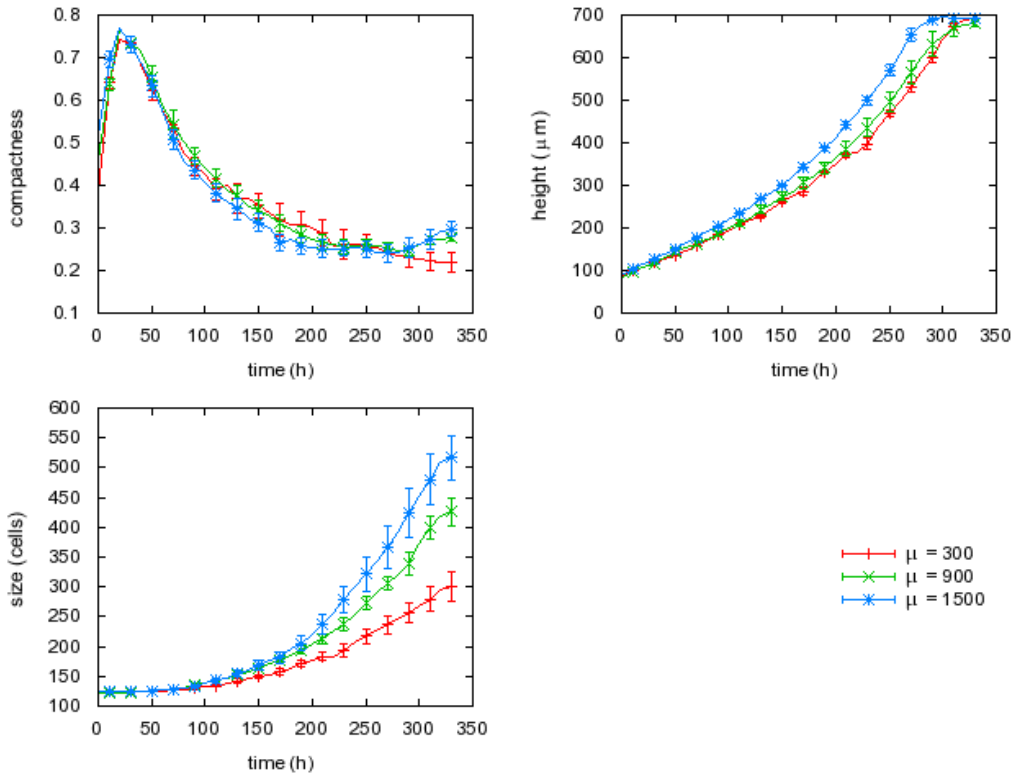

Figure 20 Compactness, height and size of the growing sprout with varying haptotaxis strength. Error bars indicate s.e.m. n = 8.

5.2.3 Haptokinesis

We next looked at haptokinesis. Here we see differences in compactness, height and size (Figure 21). If haptokinesis is set to zero, only small sprouts are formed, that do not grow much in size. For small values of haptokinesis sprouts grow very fast towards the tumor, with no or few branches. For larger values of haptokinesis strength the sprout speed decreases and more branches are formed.

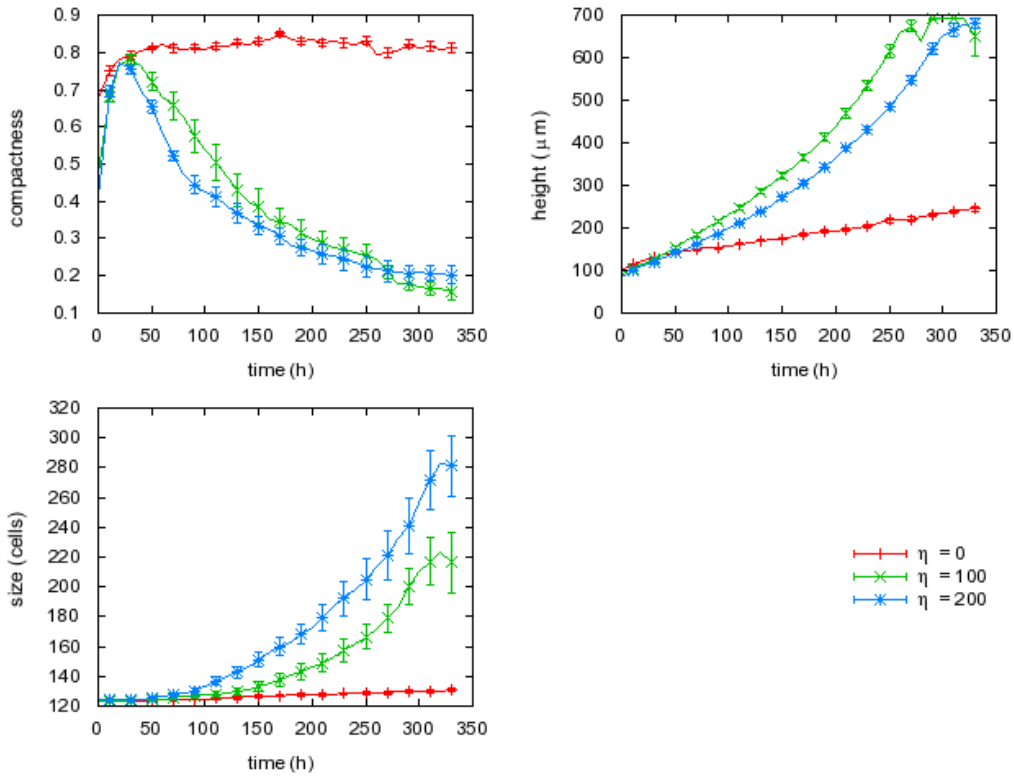

Figure 21 Compactness, height and size of the growing sprout with varying haptokinesis strength. Error bars indicate s.e.m. n = 11.

How can we explain this phenomenon? Without haptokinesis, the only mechanisms playing a role in the directional movement of cells are chemotaxis and haptotaxis. The VEGF gradient will stimulate cells to move towards the tumor, but apparently more is needed to form a growing sprout. When haptokinesis is 'switched on', but with a low strength, a sprout can be formed, and the relatively high chemotaxis strength will pull the sprout fast towards the tumor. With increasing haptokinesis, the migration forward through high ECM densities is more constrained, resulting in an increase in branching and a slower growing sprout (Figure 22).

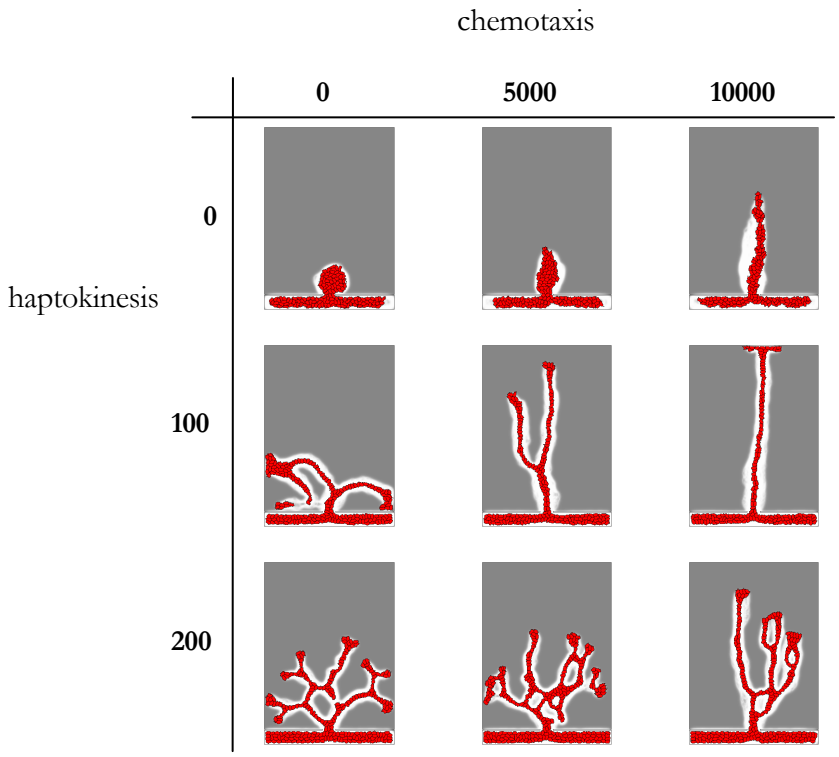

Figure 22 Examples of growing sprouts after 30000 MCS with different values of chemotaxis and haptokinesis strength.

5.2.4 Degradation of ECM by MMPs

Next we investigated the role of proteolysis, the degradation of ECM components by MMPs. Varying the decay rate of ECM affects the compactness, height and size of the sprout (Figure 23 and Figure 24).

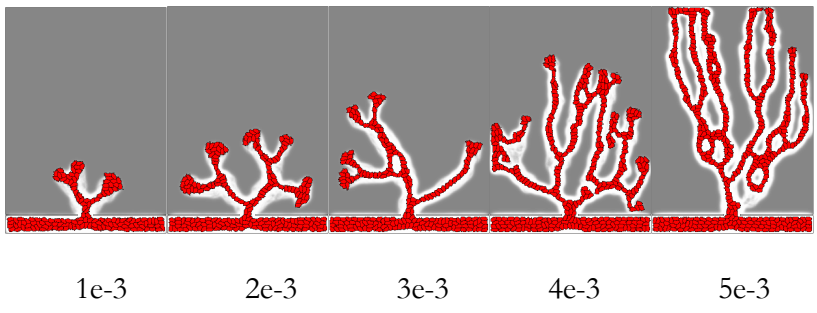

Figure 23 Examples of growing sprouts after 30000 MCSs with different ECM decay rates (subscripts).

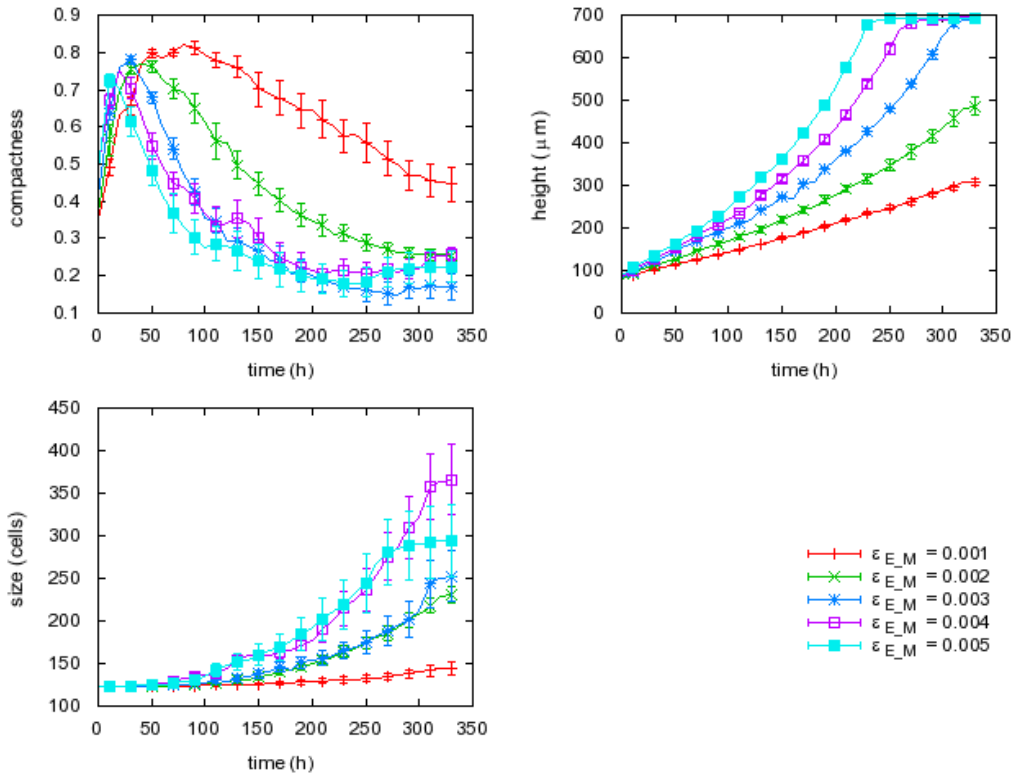

Figure 24 Compactness, height and size of the growing sprout with varying ECM decay rates. Error bars indicate s.e.m. n = 7.

A low decay rate results in small compact sprouts that grow slowly towards the tumor. Increasing the decay rate produces fast growing vascular networks with a lot of branches. Variations in secretion rate of MMPs will have similar effects (results not shown).

5.2.5 Variation in VEGF gradient

We also varied the VEGF gradient, by varying the decay rate of VEGF, to see what the effect of a shallow or steep gradient will be. In all simulations the VEGF concentration in the parent vessel is set to the same value (0.05) to ensure that cells start from the same initial situation (Figure 26).

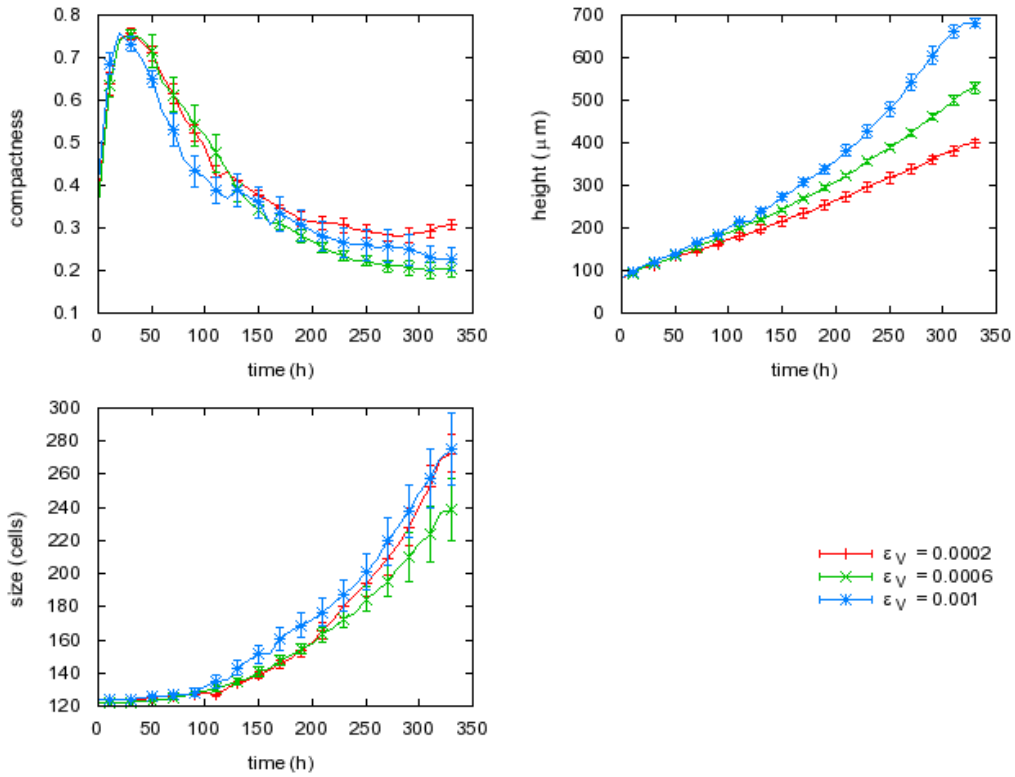

Figure 25 Compactness, height and size of the growing sprout with varying VEGF decay rates. Error bars indicate s.e.m. n = 7.

Figure 25 shows an increased sprout speed for steeper gradients. However, a steep VEGF gradient causes a higher VEGF concentration in the dish, which in turn induces MMP induction. Therefore these results should for a large part be ascribed to increased proteolysis.

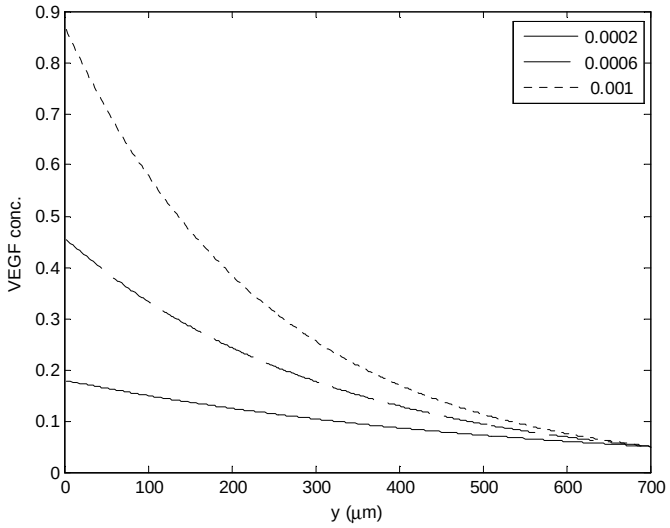

Figure 26 Increasing VEGF decay rates will establish steeper gradients.

5.2.6 Sprout formation without proliferation

When we do not allow cells to proliferate, branching sprouts are formed, however they grow must slower and parts of the sprout split off. The sprout will not reach the tumor (Figure 27 and Figure 28).

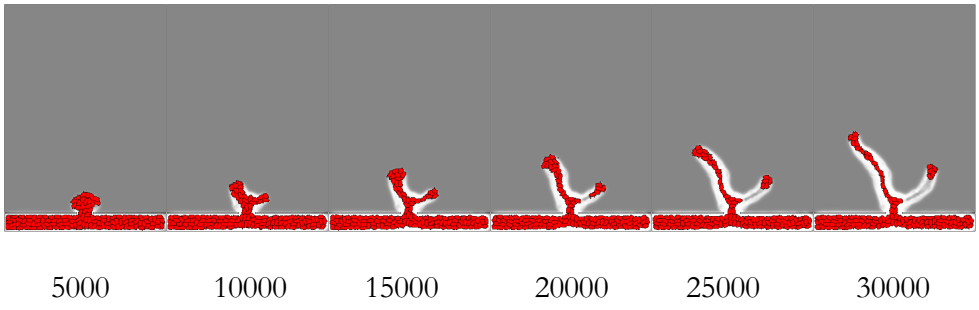

Figure 27 Example of a growing sprout without proliferation.. Subscripts: number of MCS. ECM decay rate ε_{E_M} = 2e-3, other parameters as indicated in Table 1.

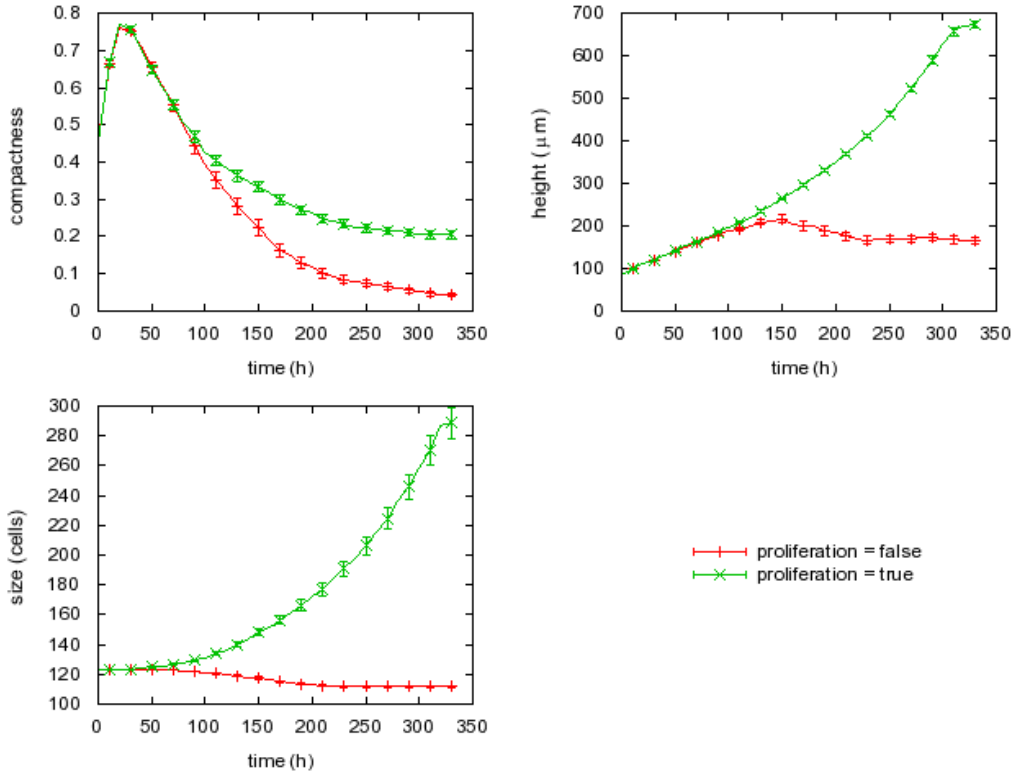

Figure 28 Compactness, height and size of the growing sprout with and without proliferation. Error bars indicate s.e.m. n = 40.

Chapter 6

Discussion

We demonstrated that our model, which describes cell-matrix interactions on the level of individual cells, is able to reproduce sprouting and branching behavior during angiogenesis. Most models that were discussed in chapter 3 needed specific branching rules to form vascular trees. Our simulation results show that our model can reproduce branching sprouts and networks, without including such specific rules.

We can conclude from our sensitivity analysis that haptokinesis, the sensitivity of cells to ECM densities, and proteolysis, the degradation of ECM components, seem to play a key role in angiogenesis. Neither chemotactic migration nor haptotaxis alone appear to be sufficient mechanisms to form stable vascular sprouts. Their role appears to be more a supporting one; chemotaxis guides the growing sprout towards the tumor and haptotaxis promotes branch formation by stimulating lateral migration of the sprout.

6.1 Comparing results with experimental observations

We can validate our model when we compare our results with experimental observations.

6.1.1 MMPs are essential for angiogenesis

In our model proteolysis is required to form growing sprouts. Without ECM degradation cells cannot invade the matrix. This is in agreement with studies that demonstrate that MMPs are essential for cell migration through 3D collagen matrices [33].

6.1.2 The steepness of the VEGF gradient

The spatial distribution of VEGF has several influences on angiogenesis. In a shallow VEGF gradient, tip cells will extend short undirected filopodia, resulting in a slow and undirected growth of sprouts. Shallow gradients will stimulate proliferation of stalk cells. Steeper VEGF gradients lead to excessive branching of vessels [7].

In our simulations with different VEGF gradients we see an increase in the speed of the sprout for steeper gradients. However, as discussed before, this must partly be ascribed to increased proteolysis. If we look at the effect of varying chemotaxis strength, which is similar to varying the VEGF gradient, we again see an increase in the speed of the sprout, but no change in branching frequency.

6.1.3 How fast do sprouts grow?

Many in vitro experiments observe that sprouts grow with a speed of ~ 1 mm in three days. This is about five times faster than our experiments. However other experiments [8] mention 10-12 days for sprouts to form and reach a tumor and this is in agreement with our observations.

In vivo and in vitro experiments show that the speed of a sprout increases when it approaches the tumor [39]. In our simulations sprouts accelerate also when they approach the tumor. This can be ascribed to the increased secretion of MMPs due to higher VEGF concentrations.

6.1.4 Cell migration and proliferation

Experiments show that both EC migration as well as proliferation plays a role in the formation of vessel sprouts. If proliferation is inhibited sprouts can form, but will not reach the tumor [10]. Our simulations agree with this, in the first phase of angiogenesis the growth of the sprout is mainly caused by migrating cells, in a later stage proliferation is responsible for sprout growth. Furthermore, we have shown that without proliferation we can reproduce branching sprouts which remain small in size.

6.1.5 Proteolysis

Although we can question whether the endured secretion of MMPs by all cells and the subsequent degradation around the sprout is realistic, classic descriptions of extracellular proteolytic activity during angiogenesis, talk about capillary sprouts surrounded with a clear space, resulting from the dissolvement of fibrin [34]. In our model this 'empty space' along the stalk of the sprout is one of the main reasons for

the formation of small and stable sprouts. Cells are not likely to move away from the sprout towards very low ECM densities.

6.1.6 Brush-border effect

A typical phenomenon in sprouting angiogenesis is the 'brush-border' effect. In the proximity of the tumor the branching of sprouts will increase resulting in a dense vascular tree [39]. In our simulations we see an increase in branching half way the dish, but when the sprouts move further, they accelerate and move to the tumor in a straight line. We assume that this is due to stronger chemotaxis and to the increase in proteolysis caused by higher VEGF concentrations.

The 'brush-border' effect could be caused by increasing stalk cell proliferation and tip cell selection induced by higher VEGF concentrations near the tumor. These phenomena are not incorporated in our model.

According to the hypothesis of Yin and coworkers [44], increased ECM degradation near the tumor will decrease the haptokinetic and haptotactic effects on cell migration. As a result cells lose the ability to follow the ECM traces left by other cells, which results in increased branching. In our model the ECM density at cell sites is rather constant, and therefore migrating cells can follow ECM cues, even near the tumor.

Chapter 7

Future work

Improvements can certainly be made to our model. We will discuss a number of them in this chapter. However, when adding new rules and restrictions to the model, it will loose its simplicity, which is in part one of its charms.

7.1 Adding tip and stalk cell behavior

We can make our model more realistic by introducing two cell types: tip cells and stalk cells. Tip cells are more motile; they lead the sprout, navigate by extending filopodia, and invade the ECM by releasing proteases. Stalk cells follow the tip cells, they are less active, proliferate and secrete ECM components. In our current model all cells are sensitive to chemotactic and haptotactic cues, they can all proliferate and secrete MMPs and ECM components. It would make the model more realistic when we divide those tasks between tip cells and stalk cells.

7.2 Proliferation induced by VEGF

Proliferation is induced by VEGF, so we could improve the model not only by restricting proliferation to stalk cells, but also by increasing the probability of cell division with higher VEGF concentrations.

7.3 Improving model of cell-matrix interactions

Although we intensively studied ways to model the cell-matrix interactions, improvements can certainly be made. For example, in our current model we don't make a distinction between the front and rear of a cell, while in reality migrating cells do have polarity. When cells preferably extend protrusions at their front persistence will be much higher.

We studied three explanations of haptokinesis: the detachment theory, receptor saturation and altered signaling and finally implemented the latter in our model of

angiogenesis. However, we think that all three theories (and maybe others) play a role in haptokinesis and it would be interesting to look further into the underlying mechanisms.

In our model degradation of ECM proteins is not regulated in the sense that the secretion of MMPs and the degradation of ECM by MMPs are not related to the ECM density in the direct environment of the cell. However, in reality, cells can fine-tune proteolysis to prevent excessive break down of the matrix. We could therefore add functionality to the model that inhibits or limits proteolysis when ECM densities are low enough for invasion.

Other mechanisms that influence the migration of cells could be included in the model. For instance shear stress, matrix rigidity and the direction of matrix fibers, can all guide cells when migrating into the matrix. Cells in their turn can remodel the fibers in the ECM leaving cues for following cells.

7.4 Improving the representation of the ECM

The ECM is now modeled as a field with initially a uniform concentration of ECM components. In reality the matrix is heterogeneous with irregular concentrations of different molecules. In our model we do not make any distinction between different ECM proteins, we generally refer to ECM components and don't have in particular collagen, fibronectin in mind. Including these distinct components with their specific properties will also make the model more realistic.

We could furthermore add matrix bound factors to the ECM, such as certain VEGF isoforms, which can be released or activated by MMPs. These factors will set up steep local gradients and this will certainly affect cell migration [33].

7.5 Quantitative validation

Most of our model parameters have no relation with physical parameters, and therefore a quantitative validation of the model is difficult. In order to make our model more realistic, we could for instance use realistic concentrations of VEGF, MMPs and ECM densities. Other values of interest are measurements concerning proteolysis, such as the induction of MMPs by VEGF or the degradation of ECM components by MMPs. Are these relations linear, like in our model?

Measurements on growing and branching sprouts could help to make our model more realistic. For example, if we would have more quantitative data from experimental observations relating to the effect of VEGF gradients and ECM densities and gradients on sprout growth and branching, we could use this information to further calibrate our model

We could use existing imaging analysis tools to measure for example the number and length of branches in a sprout. The same tools can be used to analyze images from in vitro or in vivo experiments. This way we can better compare our results with experimental observations.

.

Bibliography

1. Carmeliet, P., *Angiogenesis in life, disease and medicine.* Nature, 2005. **438**(7070): p. 932-6.

2. Carmeliet, P. and R.K. Jain, *Angiogenesis in cancer and other diseases.* Nature, 2000. **407**(6801): p. 249-57.

3. Folkman, J., *Angiogenesis: an organizing principle for drug discovery?* Nat Rev Drug Discov, 2007. **6**(4): p. 273-86.

4. Merks, R.M.H. and J.A. Glazier, *A cell-centered approach to developmental biology.* Physica a-Statistical Mechanics and Its Applications, 2005. **352**(1): p. 113-130.

5. Folkman, J. and M. Klagsbrun, *Angiogenic factors.* Science, 1987. **235**(4787): p. 442-7.

6. Liao, D. and R.S. Johnson, *Hypoxia: a key regulator of angiogenesis in cancer.* Cancer Metastasis Rev, 2007. **26**(2): p. 281-90.

7. Gerhardt, H., *VEGF and endothelial guidance in angiogenic sprouting.* Organogenesis, 2008. **4**(4): p. 241-6.

8. Ausprunk, D.H. and J. Folkman, *Migration and proliferation of endothelial cells in preformed and newly formed blood vessels during tumor angiogenesis.* Microvasc Res, 1977. **14**(1): p. 53-65.

9. Fantin, A., et al., *Tissue macrophages act as cellular chaperones for vascular anastomosis downstream of VEGF-mediated endothelial tip cell induction.* Blood, 2010.

10. Paweletz, N. and M. Knierim, *Tumor-related angiogenesis.* Crit Rev Oncol Hematol, 1989. **9**(3): p. 197-242.

11. Phng, L.K. and H. Gerhardt, *Angiogenesis: a team effort coordinated by notch.* Dev Cell, 2009. **16**(2): p. 196-208.

12. De Smet, F., et al., *Mechanisms of vessel branching: filopodia on endothelial tip cells lead the way.* Arterioscler Thromb Vasc Biol, 2009. **29**(5): p. 639-49.

13. Gerhardt, H., et al., *VEGF guides angiogenic sprouting utilizing endothelial tip cell filopodia.* J Cell Biol, 2003. **161**(6): p. 1163-77.

14. Hunter, W.L. and A.L. Arsenault, *Vascular invasion of the epiphyseal growth plate: analysis of metaphyseal capillary ultrastructure and growth dynamics.* Anat Rec, 1990. **227**(2): p. 223-31.

15. Kearney, J.B., et al., *The VEGF receptor flt-1 (VEGFR-1) is a positive modulator of vascular sprout formation and branching morphogenesis.* Blood, 2004. **103**(12): p. 4527-35.

16. Sainson, R.C., et al., *Cell-autonomous notch signaling regulates endothelial cell branching and proliferation during vascular tubulogenesis.* FASEB J, 2005. **19**(8): p. 1027-9.

17. Alberts, B., et al., *Molecular Biology of the cell.* 5 ed. 2008, Newyork: Garland Science.

18. Davis, G.E. and D.R. Senger, *Endothelial extracellular matrix: biosynthesis, remodeling, and functions during vascular morphogenesis and neovessel stabilization.* Circ Res, 2005. **97**(11): p. 1093-107.

19. Lamalice, L., F. Le Boeuf, and J. Huot, *Endothelial cell migration during angiogenesis.* Circ Res, 2007. **100**(6): p. 782-94.

20. Li, S., J.L. Guan, and S. Chien, *Biochemistry and biomechanics of cell motility.* Annu Rev Biomed Eng, 2005. **7**: p. 105-50.

21. Barkefors, I., et al., *Endothelial cell migration in stable gradients of vascular endothelial growth factor A and fibroblast growth factor 2: effects on chemotaxis and chemokinesis.* J Biol Chem, 2008. **283**(20): p. 13905-12.

22. Senger, D.R., et al., *The alpha(1)beta(1) and alpha(2)beta(1) integrins provide critical support for vascular endothelial growth factor signaling, endothelial cell migration, and tumor angiogenesis.* Am J Pathol, 2002. **160**(1): p. 195-204.

23. Smith, J.T., et al., *Measurement of cell migration on surface-bound fibronectin gradients.* Langmuir, 2004. **20**(19): p. 8279-86.

24. Smith, J.T., J.T. Elkin, and W.M. Reichert, *Directed cell migration on fibronectin gradients: effect of gradient slope.* Exp Cell Res, 2006. **312**(13): p. 2424-32.

25. Wu, P., et al., *Integrin-binding peptide in solution inhibits or enhances endothelial cell migration, predictably from cell adhesion.* Ann Biomed Eng, 1994. **22**(2): p. 144-52.

26. Cox, E.A., S.K. Sastry, and A. Huttenlocher, *Integrin-mediated adhesion regulates cell polarity and membrane protrusion through the Rho family of GTPases.* Mol Biol Cell, 2001. **12**(2): p. 265-77.

27. DiMilla, P.A., et al., *Maximal migration of human smooth muscle cells on fibronectin and type IV collagen occurs at an intermediate attachment strength.* J Cell Biol, 1993. **122**(3): p. 729-37.

28. Palecek, S.P., et al., *Integrin-ligand binding properties govern cell migration speed through cell-substratum adhesiveness.* Nature, 1997. **385**(6616): p. 537-40.

29. Gaudet, C., et al., *Influence of type I collagen surface density on fibroblast spreading, motility, and contractility.* Biophys J, 2003. **85**(5): p. 3329-35.

30. Chon, J.H., et al., *Alpha4beta1 and alpha5beta1 control cell migration on fibronectin by differentially regulating cell speed and motile cell phenotype.* Ann Biomed Eng, 1998. **26**(6): p. 1091-101.

31. Zaman, M.H., et al., *Migration of tumor cells in 3D matrices is governed by matrix stiffness along with cell-matrix adhesion and proteolysis.* Proc Natl Acad Sci U S A, 2006. **103**(29): p. 10889-94.

32. DiMilla, P.A., K. Barbee, and D.A. Lauffenburger, *Mathematical model for the effects of adhesion and mechanics on cell migration speed.* Biophys J, 1991. **60**(1): p. 15-37.

33. van Hinsbergh, V.W. and P. Koolwijk, *Endothelial sprouting and angiogenesis: matrix metalloproteinases in the lead.* Cardiovasc Res, 2008. **78**(2): p. 203-12.

34. Pepper, M.S., *Role of the matrix metalloproteinase and plasminogen activator-plasmin systems in angiogenesis.* Arterioscler Thromb Vasc Biol, 2001. **21**(7): p. 1104-17.

35. Haas, T.L. and J.A. Madri, *Extracellular matrix-driven matrix metalloproteinase production in endothelial cells: implications for angiogenesis.* Trends Cardiovasc Med, 1999. **9**(3-4): p. 70-7.

36. Haas, T.L., S.J. Davis, and J.A. Madri, *Three-dimensional type I collagen lattices induce coordinate expression of matrix metalloproteinases MT1-MMP and MMP-2 in microvascular endothelial cells.* J Biol Chem, 1998. **273**(6): p. 3604-10.

37. Chun, T.H., et al., *MT1-MMP-dependent neovessel formation within the confines of the three-dimensional extracellular matrix.* J Cell Biol, 2004. **167**(4): p. 757-67.

38. Hawinkels, L.J., et al., *VEGF release by MMP-9 mediated heparan sulphate cleavage induces colorectal cancer angiogenesis.* Eur J Cancer, 2008. **44**(13): p. 1904-13.

39. Mantzaris, N.V., S. Webb, and H.G. Othmer, *Mathematical modeling of tumor-induced angiogenesis.* J Math Biol, 2004. **49**(2): p. 111-87.

40. Anderson, A.R. and M.A. Chaplain, *Continuous and discrete mathematical models of tumor-induced angiogenesis.* Bull Math Biol, 1998. **60**(5): p. 857-99.

41. Levine, H.A., B.D. Sleeman, and M. Nilsen-Hamilton, *Mathematical modeling of the onset of capillary formation initiating angiogenesis.* J Math Biol, 2001. **42**(3): p. 195-238.

42. Levine, H.A., et al., *Mathematical modeling of capillary formation and development in tumor angiogenesis: penetration into the stroma.* Bull Math Biol, 2001. **63**(5): p. 801-63.

43. Manoussaki, D., *A mechanochemical model of angiogenesis and vasculogenesis.* M2AN, 2003. **37**(4): p. 581-599.

44. Yin, Z., et al., *Analysis of pairwise cell interactions using an integrated dielectrophoretic-microfluidic system.* Mol Syst Biol, 2008. **4**: p. 232.

45. Milde, F., M. Bergdorf, and P. Koumoutsakos, *A hybrid model for three-dimensional simulations of sprouting angiogenesis.* Biophys J, 2008. **95**(7): p. 3146-60.

46. Stokes, C.L. and D.A. Lauffenburger, *Analysis of the roles of microvessel endothelial cell random motility and chemotaxis in angiogenesis.* J Theor Biol, 1991. **152**(3): p. 377-403.

47. Glazier, J.A., et al., *Coordinated action of N-CAM, N-cadherin, EphA4, and ephrinB2 translates genetic prepatterns into structure during somitogenesis in chick.* Curr Top Dev Biol, 2008. **81**: p. 205-47.

48. Merks, R.M., et al., *Cell elongation is key to in silico replication of in vitro vasculogenesis and subsequent remodeling.* Dev Biol, 2006. **289**(1): p. 44-54.

49. Savill, N.J. and P. Hogeweg, *Modelling Morphogenesis: From Single Cells to Crawling Slugs.* Journal of Theoretical Biology, 1997. **184**(3): p. 229-235.

50. Glazier, J.A. and F. Graner, *Simulation of the differential adhesion driven rearrangement of biological cells.* Phys Rev E Stat Phys Plasmas Fluids Relat Interdiscip Topics, 1993. **47**(3): p. 2128-2154.

51. Bauer, A.L., T.L. Jackson, and Y. Jiang, *A cell-based model exhibiting branching and anastomosis during tumor-induced angiogenesis.* Biophys J, 2007. **92**(9): p. 3105-21.

52. Merks, R.M., et al., *Contact-inhibited chemotaxis in de novo and sprouting blood-vessel growth.* PLoS Comput Biol, 2008. **4**(9): p. e1000163.

53. Shirinifard, A., et al., *3D multi-cell simulation of tumor growth and angiogenesis.* PLoS One, 2009. **4**(10): p. e7190.

54. Szabo, A. and A. Czirok, *The Role of Cell-Cell Adhesion in the Formation of Multicellular Sprouts.* Math Model Nat Phenom, 2010. **5**(1): p. 106.

55. Dejana, E., *Endothelial cell-cell junctions: happy together.* Nat Rev Mol Cell Biol, 2004. **5**(4): p. 261-70.

56. Wartlick, O., A. Kicheva, and M. Gonzalez-Gaitan, *Morphogen gradient formation.* Cold Spring Harb Perspect Biol, 2009. **1**(3): p. a001255.

57. Press, W.H., *Numerical recipes : the art of scientific computing.* 3rd ed. 2007, Cambridge, UK ; New York: Cambridge University Press. xxi, 1235 p.

58. Hogeweg, P., *Evolving mechanisms of morphogenesis: on the interplay between differential adhesion and cell differentiation.* J Theor Biol, 2000. **203**(4): p. 317-33.

59. Zeng, G., et al., *Orientation of endothelial cell division is regulated by VEGF signaling during blood vessel formation.* Blood, 2007. **109**(4): p. 1345-52.

60. Doyle, J. and R.L. Rivest, *Linear expected time of a simple union-find algorithm.* Information Processing Letters, 1976. **5**(5): p. 146-148.